Global Planning for Dextrous Re-orientation of Rigid Objects: Finger Tracking with Rolling and Sliding

Moëz Cherif, Kamal K. Gupta

INSTITUT NATIONAL DE RECHERCHE EN INFORMATIQUE ET EN AUTOMATIQUE

Global Planning for Dextrous Re-orientation of Rigid Objects: Finger Tracking with Rolling and Sliding

Moëz Cherif and Kamal K. Gupta

N ° 3770

Septembre 1999

THÈME 3

ISSN 0249-6399

Global Planning for Dextrous Re-orientation of Rigid Objects: Finger Tracking with Rolling and Sliding

Moëz Cherif* and Kamal K. Gupta†

Thème 3 — Interaction homme-machine,
images, données, connaissances
Projet Sharp

Rapport de recherche n ° 3770 — Septembre 1999 — 43 pages

Abstract: We address global motion planning for quasi-static re-orientation of convex objects (polyhedral and smooth objects) with a four-fingertip grasp. We make use of a simple human-like manipulation strategy in which a single finger is moved at each instant while the other three are maintained fixed (*w.r.t.* the palm) –an extended version of the original finger tracking scheme of Rus [25, 26]. This new version essentially incorporates frictional rolling and sliding at the fingertips and deals with the related contact kinematics and quasi-static motion/force prediction issues. Our contribution is twofold. First, we describe an analysis showing that this extended scheme is suitable for reducing the space of the object motions; thereby making motion planning easier and operating on a search space of low dimension. Our second contribution is a planner that exploits such a search space reduction and applies the extended finger tracking at the core of a multi-level hierarchical framework to search for global re-orientation trajectories. The planner has been implemented and used for achieving several non-trivial frictional re-orientation tasks that show the capabilities and the promise of our approach.

Key-words: Dextrous manipulation, motion planning, object re-orientation, fingertip grasp, kinematics, quasi-static systems, rolling and sliding contacts.

(Résumé : tsvp)

Work of M. Cherif partly done during a research appointment at Simon Fraser University. Work partly funded by a Co-operative R&D grant from Natural Sciences and Engineering Research Council of Canada (NSERC).

This report has been submitted to the International Journal of Robotics Research.

* Expert Engineer currently with the Validation System Project (VASY R-A), INRIA Rhône-Alpes. E-mail: `Moez.Cherif@inrialpes.fr`.

† Simon Fraser University, School of Engineering Science, Burnaby, B.C., V5A 1S6, Canada. E-mail: `kamal@cs.sfu.ca`.

Unité de recherche INRIA Rhône-Alpes
655, avenue de l'Europe, 38330 MONTBONNOT ST MARTIN (France)
Téléphone : 04 76 61 52 00 - International: +33 4 76 61 52 00
Télécopie : 04 76 61 52 52 - International: +33 4 76 61 52 52

Planification globale pour la ré-orientation dextre d'objets rigides : "Finger tracking" avec roulement et glissement.

Résumé : Ce papier traite du problème de la planification de mouvement pour la ré-orientation quasi-statique d'objets convexes (polyèdres et objets à surface lisse) par une main articulée à quatre doigts. Nous utilisons une stratégie de manipulation proche de celles utilisées par un opérateur humain. À tout moment, un seul doigt est contrôlé à bouger pendant que les autres doigts sont maintenus fixes par rapport à la palme de la main. Ce schéma est une version étendue du schéma original proposé par Rus [25, 26] et connu sous l'appellation anglo-saxone "finger tracking". Notre nouveau schéma, qui est plus général, prend en compte la possibilité d'effectuer la manipulation par différent type de contact (en particulier roulement et glissement en présence de frottement) et traite aussi d'aspects divers liés à la cinématique de contact et à la génération des mouvements et forces mis en jeu dans les systèmes quasi-statiques. Notre contribution est double. La première est une analyse montrant que notre schéma est adéquat pour la réduction de l'espace dans lequel doit s'effectuer la planification des mouvements admissibles de l'objet. La seconde contribution est un algorithme de planification de mouvement qui exploite ce résultat en opérant de manière hiérarchique en trois niveaux afin de trouver des trajectoires globales admissibles et utilisables pour la ré-orientation d'objets. L'algorithme de planification a été implanté et utilisé pour la résolution de plusieurs tâches de ré-orientation non-triviales qui permettent de valider notre approche en simulation et de démontrer la capabilité de notre planificateur.

Mots-clé : Manipulation dextre, planification de mouvement, ré-orientation d'objets, saisie par les bouts des doigts, cinématique, systèmes quasi-statiques, contacts de type roulement et glissement.

1 Introduction

Prehensile object manipulation by artificial multi-fingered hands has received great interest in the past. Many works focussed on the synthesis and analysis of (form- and force-) closure properties of grasps (e.g., [20, 17, 16, 1, 29]) and on the study of the mechanics and dexterity of robotics hands in a framework of instantaneous motion prediction and/or robot control (e.g., [27, 15, 8, 9, 10, 11, 2, 30, 34, 33, 35]). These works have showed in different contexts that many non-trivial geometric, mechanical, and control issues are involved in dextrous manipulation by robot hands. This makes the programming of such hands complicated, often limiting their applications to simple demonstrative tasks. We believe that global motion planning is an effective tool and a promising avenue for enhancing the present capabilities of multi-fingered hands for dextrous manipulation of objects.

An important problem in dextrous manipulation is that of in-hand object re-grasping (or, re-grasping for short). It consists of automatically moving the hand-object system between two specified grasps (configurations of the entire hand-object system) while the object is held in the hand during the entire motion. In [14], Li et al. presented a comprehensive formulation of this problem with a focus on four contact types at the fingertips: pure rolling, pure fingertip twisting (or coordinated motions), and fingertip re-location by pure sliding or breaking contact. Although they did not present algorithms to solve the problem, they discussed some properties of the solution space which gives a flavor of the fundamental difficulties inherent in the re-grasping problem. A key issue is the high dimensionality of the search space –the combined configuration space of the object and the hand– in conjunction with the complexity (combinatorial and algebraic) that arises due to different contact types.

In [6], we presented a hierarchical and structured search framework to deal with this complexity to solve a class of re-grasping problems – we called it re-configuration problem – where the goal is to achieve only a final desired configuration (position and orientation) of the object. The overall planning framework is a (interleaved) three-level process, as follows (see Fig. 1). At the top level, the object is moved independent of any constraints as if it were a free body. For instance, a possible choice is to move the object along the shortest path (w.r.t. a given metric), e.g. a straight line in the object C-space, $SE(3)$, toward the desired configuration. Knowing this nominal motion of the object, the second level solves for the corresponding finger motion (Inverse Finger Motion Problem, or for brevity, the inverse problem). Note that the governing equations for the precise system may change depending on the "strategy" (we call it manipulation mode) used. For instance, one could use all the fingers for some duration of motion [3], and then keep some of them fixed, followed by using all of them again, resulting in a different set of governing equations at different time instants. Note that humans naturally use several different "modes" while manipulating objects with their hands. Furthermore, as we will show in this paper for a particular mode, the planning process can take advantage of the effects of such strategies on the geometric structure of the search spaces and on the different levels of planning.

In this paper, we consider a further restricted version of the re-configuration, where only the desired final orientation of the object is specified (instead of the complete configuration); we call it the re-orientation problem –given an initial grasp, the re-orientation

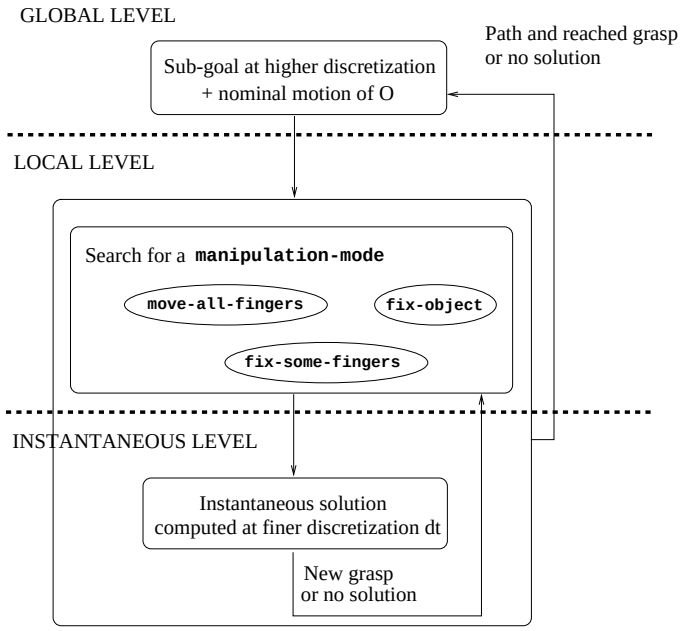

Figure 1: A schematic view of the multi-level planning algorithm.

problem consists of finding a (piece-wise) smooth dextrous trajectory (fingertips-object trajectories and contact forces) achieving a final desired orientation of the object. class of re-grasping problems when the goal is to achieve only a final desired configuration of the object (position/orientation). We explore re-orientation planning by four-fingertip grasps and applying a human-like manipulation strategy consisting, at each instant, in fixing three fingertips *w.r.t.* the palm and re-orienting the object through the motions of the fourth fingertip. Such a strategy, called also "finger tracking", has been previously used by Rus [25, 26] for polyhedral objects in the absence of friction and when the fingertips are points (see also the following discussion of related works). Rus has showed that for polyhedra, the finger tracking strategy enables to show that the object C-space is locally diffeomorphic to $SO(3)$. We further show that finger tracking yields a *global* diffeomorphism between the object C-space and $SO(3)$. Our analysis is presented for convex objects including smooth objects and polyhedra. §4 presents this analysis. Our second contribution is an algorithm that solves a *quasi-static* version of the above-stated re-orientation problem for 3-D convex rigid objects, polyhedral as well as smooth objects. The algorithm exploits the above-mentioned global property to search for the object trajectories within a subset of $I\!R^3$ (parameterizing $SO(3)$) while dealing with the system redundancy and taking into account numerous constraints of dextrous manipulation ; contact kinematics, different contact modes such as rolling or

sliding, non-linearity of friction constraints, no-collision between the fingertips, reachability and equilibrium of grasps.

2 Related Work

Fearing demonstrated planar re-orientations of a baton (by twirling) with the three-fingered Stanford/JPL hand [10, 11]. His work was more focussed on the implementation of tactile sensing. Twirling was performed in two sequential steps: (1) re-orienting the object by pushing it with a single moving fingertip while the two others are (almost) fixed and maintain the baton in equilibrium, and (2) re-grasping the baton by re-locating the pushing fingertip through breaking contacts. No planning was addressed in this work. In a similar context, Brock considered sliding contacts (he called it controlled sliding) for instantaneous object re-orientation about arbitrary axes [2] (See also the work of Payandeh [23]).

More recently, Rus used finger tracking for re-orienting polyhedra, by four frictionless point fingertips [25, 26]. A single fingertip is moved on the face of the polyhedron (i.e., it tracks the motion of the polyhedron) while the other three are fixed (*w.r.t.* the palm frame). She showed that the space of possible object configurations is (at each instant) diffeomorphic to the three-dimensional rotation space ($SO(3)$). This is because maintaining the contact at fixed fingertips corresponds to (at each instant) constraints in the object configuration space ($SE(3)$), effectively reducing the space of possible motions. This means that for a given set of fixed fingertips and a given orientation of the object, there exists a unique corresponding position in the workspace (hence a unique configuration in $SE(3)$). A second elegant result is that with frictionless contacts, the dynamic equations, at each instant, are linear in the (translation) displacement parameters of the object, and in the contact position/force of the moving fingertip. Therefore, the instantaneous motion (axis of rotation) of the object is uniquely determined from the contact positions and the forces applied, and vice-a-versa. Although Rus addressed some planning issues, her framework is local since it does not cope with breaking contacts when crossing the polyhedron edges and does not explicitly search for the object trajectory. Exploiting Rus's results, Gupta [12] presents a global planner for re-orienting a polyhedral object by finger tracking. The planner searches a tree of landmarks placed randomly in $SO(3)$. The planner makes the same assumptions as in Rus's work – point fingertips so that contact kinematics do not arise, only pure sliding motion (no rolling), polyhedral objects. In addition, the fixed fingertips are chosen once before planning and are assumed to lie on different faces with no switching of fingers from one face to another.

A few other works have addressed global re-orientation motion planning. Trinkle and Paul [32] presented an algorithm for quasi-static re-orientation of polygons in the plane by power (whole-finger) grasps with sliding contacts. The algorithm has not been extended for 3-D manipulation. Trinkle and Hunter [31] described a framework for planning global motions for a sliding polygonal workpiece manipulated in the plane but did not present any implementation. In the 3-D case, Omata et al. [22, 21] applied a strategy similar to that of Fearing for addressing purely geometric gross manipulation planning in the absence of

kinematic and friction constraints. We cope with kinematics and friction and our model of contact is more realistic.

Many of these works motivated us for addressing the re-orientation problem using an opportunistic (human-like) manipulation strategy. We extend finger tracking to smooth objects, incorporate contact kinematics (rolling and sliding with non-point fingertips), and adapt it to quasi-static manipulation motions which accounts for friction and reachability of fingertips. Note that in Rus work, the fingertips are points and the contacts are frictionless. We use the resulting extended manipulation strategy at the core of a global planning framework to plan dextrous re-orientation of objects held within a four-fingertip grasp. Our planner is able to deal with face boundaries for the case of polyhedral objects.

3 Problem Statement

3.1 General assumptions

Our first assumption is that all the geometric and physical features of the interacting bodies are well-known and that the effects of uncertainty can be neglected. We concentrate on convex rigid bodies and on precise manipulation by four-fingertip grasps (i.e., the four contacts are points). For this purpose, we consider an idealized effector by reducing the hand to the set of its fingertips and by constraining each of them to lie in a specified finite workspace (e.g., the full set or a subset of the positions/orientations the fingertips can reach). (See Fig. 2). We consider rigid bodies assuming that the area of contact is small enough compared to the object and fingertip sizes and that it can be reduced to a point model. We investigate the application of the fingertip tracking strategy considering, at each instant, that only pure rolling is considered at the moving fingertip and that rolling, sliding, and twisting can be combined at the fixed fingertips. We use the same definition for pure rolling as [14]. In addition, we consider a quasi-static analysis to predict the motion and the contact forces of the system. This is motivated by the fact that precise manipulation often requires slow displacements of the fingertips-object system with the interaction forces dominating inertial terms. From a computational perspective, neglecting dynamic effects has the advantage of avoiding posing the planning problem in the state space of the full system (a high dimensional space since the fingertips-object system C-space is very large).

3.2 Notation

Let O denotes the manipulated object (a polyhedra or a smooth object), and let F_i be a fingertip. We denote the surfaces of O and F_i by ∂O and ∂F_i, respectively. As shown in Fig. 2, we attach at each body X (O or F_i) a frame $\mathcal{F}_X$, having each origin at the center of mass of X. The configuration of X is denoted by $g_X = (r_X, R_X) \in SE(3)$, where r_X and R_X are the position vector and rotation matrix of $\mathcal{F}_X$ *w.r.t.* a fixed reference frame, $\mathcal{F}_P$, attached in the environment ($\mathcal{F}_P$ is located in general on the palm if the complete hand is modeled). The C-space, CS_X, of X is $SE(3)$. When needed, we locally parameterize

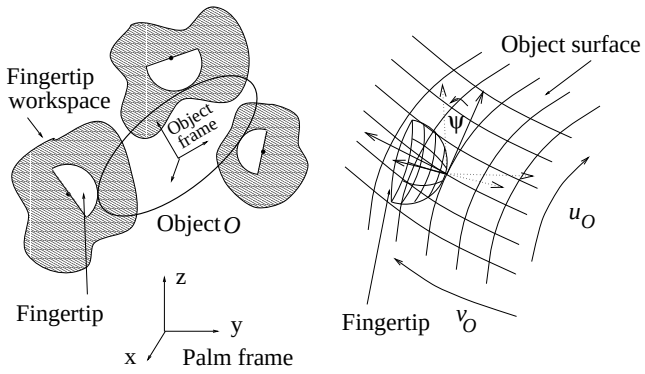

Figure 2: Left: the idealized fingertips-object system where the kinematic constraints of the (real) finger chains are replaced by finite reachability regions for the fingertips. Right: the contact frames ; $\mathcal{F}_{c_i,O}$ (solid) and $\mathcal{F}_{c_i,F_i}$ (dotted).

the rotation of X by the yaw/roll/pitch orientation angles corresponding to R_X. *Wlog*, k denotes the number of fingertips (in this paper, $k = 4$). Hence, the C-space, CS, of the entire manipulation system is $SE(3)^{k+1}$. A grasp $\mathbf{g} = (g_O, g_{F_1}, \ldots, g_{F_k})$ is an element of CS.

We define locally the configuration of each contact by $\eta_i = (\eta_{i,O}, \eta_{i,F_i}, \psi_i)^T$, where $\eta_{i,O} = (u_{i,O}, v_{i,O})$ and $\eta_{i,F_i} = (u_{F_i}, v_{F_i})$ are the position parameters of c_i on the surfaces ∂O and ∂F_i, respectively, and ψ_i is the angle between the x axes of two Gaussian frames, $\mathcal{F}_{c_i,O}$ and $\mathcal{F}_{c_i,F_i}$, attached on ∂O and ∂F_i, respectively (see Fig. 2) [18]. For a polyhedron and for a given face, ∂O_j, $\mathcal{F}_{c_i,O}$ is obtained by translating a frame fixed on the centroid o_j of ∂O_j to the contact c_i. We denote the configuration of $\mathcal{F}_{c_i,O}$ *w.r.t.* $\mathcal{F}_O$ and the configuration of $\mathcal{F}_{c_i,F_i}$ *w.r.t.* $\mathcal{F}_{F_i}$ by $g_{c_i,O} = (r_{c_i,O}, R_{c_i,O})$ and $g_{c_i,F_i} = (r_{c_i,F_i}, R_{c_i,F_i})$, respectively.

3.3 The Problem

The re-orientation problem is formally stated as follows:

> *Given an initial k-fingertip grasp configuration,* $\mathbf{g}_{start}$ *(a point in* CS*, with* $k = 4$*), and an orientation of* O *specified by an orientation,* $R_{O,goal}$*, in* $SO(3)$*, find a feasible (piecewise-) smooth trajectory,* Γ *in* CS*, and the corresponding contact forces* f *that take the fingertips-object system from* $\mathbf{g}_{start} = \Gamma(0)$ *to a grasp,* $\mathbf{g}$*, in a finite period of time,* t_f*, such that* $R_O(t_f) = R_{O,goal}$*, i.e.,* $\Gamma(t_f)$ *is within the set of grasps* $\mathbf{g} \in I\!R^3 \times \{R_{O,goal}\} \times SE(3)^k$.

4 Geometric analysis of the search space

We now discuss the effect of the instantaneous re-orientation strategy – fixing 3 fingertips and moving only the remaining one(s) – on the structure of the C-space, CS_O, of O. We consider both the case of polyhedra and convex smooth 3-D objects manipulated by spherical fingertips F_i of radius ρ_i. We illustrate our presentation by considering 2-D manipulation tasks performed by three-fingertip grasps when two fingertips are, at each instant, fixed. We denote by $CS_O(d)$ the C-space of O ($d = 2$ or 3 in the 2-D or 3-D case, respectively). For a simple presentation, we consider that the fingertips are always numbered such that $F_m,\ m = d+1$, denotes the moving fingertip, and the fixed ones are $F_i,\ i = 1 \ldots d$.

4.1 Case of a polyhedron

4.1.1 Local property of CS_O

Rus [25] has already shown that CS_O is locally diffeomorphic to $SO(3)$ for a tetrahedron, and the result is trivially extended for a general polyhedron. We outline the development here briefly. *Wlog*, we assume that each F_i is initially in contact with the face ∂O_i implying that there exists a unique intersection point c_i between them. Since the fingertips are spherical, the center of each F_i is, at each instant, on the boundary of an enlarged (generalized, since it may have curved edges) polygon, O', as shown in Fig. 3 for the 2-D case. Let o'_i be the centroid of $\partial O'_i$. A contact exists between F_i and ∂O_i (hence the position r_{F_i} lies on $\partial O'_i$) if the normal n_i and the vector connecting o'_i to r_{F_i} are perpendicular (*w.r.t.* the frame $\mathcal{F}_O$). We then have the system of constraints

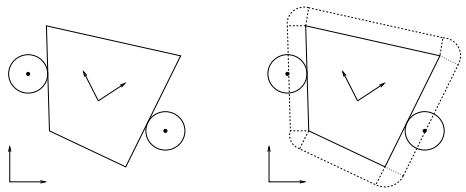

Figure 3: A 2-D case. Left: a polygon O contacted by two fixed circular fingertips having the same radii. Right: the generalized polygon resulting from enlarging O.

$$(R_O^{-1} r_{F_i} - R_O^{-1} r_O - o'_i) \,.\, n_i = 0\ ,\quad i = 1 \ldots 3 \tag{1}$$

which has a unique solution if the normals n_1, n_2, and n_3 are not co-planar, in which case r_O has the form $r_O(R_O) = \alpha_1 n_1 + \alpha_2 n_2 + \alpha_3 n_3$, where α_1, α_2, and α_3 depend on R_O and r_{F_i}, and can be deduced from (1). This means that the position r_O of O is completely defined in term of its current orientation R_O (and the r_{F_i}'s and the n_i's, $i = 1 \ldots 3$). One can now invoke inverse function theorem (as in [25]) to show that a diffeomorphism exists between $CS_o(d)$ and $SO(d)$.

We can state the following local property: *For a given grasp* $\mathbf{g^0}$ *(including the orientation* R_O^0 *of* O*) and knowing the fixed* F_i*'s,* $i = 1 \ldots d$*, and the three faces in contact with them,* $CS_O(d)$*,* $d = 2, 3$*, is locally diffeomorphic to* $SO(d)$ *at* R_O^0 *if the normals to the faces in contact with the fixed* F_i*'s are linearly independent and the contact points* $c_{i,O}^0$*,* $i = 1 \ldots d$ *are strictly in the interior of the corresponding faces (i.e.,* $c_{i,O}^0$ *are not located on the edges or the vertices of* O*).*

4.1.2 Global property of CS_O

We now show that $SO(d)$, $d = 2, 3$ is globally diffeomorphic to $CS_O(d)$. Our development is new since the earlier work [25] considered only the property of local diffeomorphism with the condition that all the fingertips remain in contact with the same faces.

Let consider a local parameterization of $SO(d)$ and $SE(d)$ based on the yaw/roll/pitch orientation angles corresponding to the rotation matrices. For the same set of fixed fingertips, let $\mathcal{R}$ be the range of orientations satisfying the local condition in §4.1.1. $\mathcal{R}$ is an open subset of $I\!R^{\frac{d(d-1)}{2}}$ since the orientations where the contacts are on the edges or the vertices of the polyhedron are not valid. Let S be the open region of $SO(d)$ which is locally parameterized by $\mathcal{R}$. We already know that $SO(d)$ is locally diffeomorphic to $CS_O(d)$ at $R_O \in S$. Showing that $SO(d)$ is globally diffeomorphic to $CS_O(d)$ is based on constructing a collection of open regions S_j covering $SO(d)$ where each S_j is globally diffeomorphic to $CS_O(d)$. In other words, we have to construct an atlas between $SO(d)$ and $CS_O(d)$ where the charts are the diffeomorphism between the S_j's and $CS_O(d)$. For constructing the S_i's, we consider the corresponding range domains $\mathcal{R}_j$. Starting from an initial grasp (including the set of fixed fingertips) and having characterized the corresponding range $\mathcal{R}_1$, our conjecture is based on the fact that by changing the set of fixed fingertips (hence the locations of the fixed fingertips *w.r.t.* $\mathcal{F}_P$), a new set of orientations of O can be made reachable. Some of these orientations are not in $\mathcal{R}_1$ and are used to construct a new range $\mathcal{R}_2$ such that $\mathcal{R}_2 \cap \mathcal{R}_1 \neq \emptyset$ and $\mathcal{R}_2 \cup \mathcal{R}_1 \neq \mathcal{R}_1$. Using $\mathcal{R}_2$, a new set, $\mathcal{R}_3$, of reachable orientations can be similarly obtained by changing the set of fixed fingertips. This scheme is iterated until the whole orientation space is covered by the $\mathcal{R}_j$'s. In this case, the corresponding open regions S_j also cover $SO(d)$ and the set of corresponding charts is considered to obtain the property of global diffeomorphism between $SO(d)$ and $CS_O(d)$.

We first consider the 2-D case to give a flavor of the construction of the $\mathcal{R}_j$'s. let us consider the polygon depicted in Fig. 3. Although there might be several schemes for changing the grasps (including moving the fingertips between adjacent faces) and constructing the $\mathcal{R}_j$'s, we pick and consider a very simple scenario. Let $\mathcal{R}_1$ be the characterized range using the initial grasp $\mathbf{g}_{start}$ shown on the top of Fig. 4. $\mathcal{R}_1$ is obtained by moving O clockwise and counter-clockwise until a fixed fingertip is in contact with a vertex. Since such contact configurations are considered as singular (because the system (1) is ill-defined), $\mathcal{R}_1$ is defined by an open interval of orientation angles having its limits at the orientations corresponding to the two possible singular grasps (see middle of Fig. 4). (We consider that F_3 (the black fingertip in the initial grasp) remains at the same position on O during its motion). The

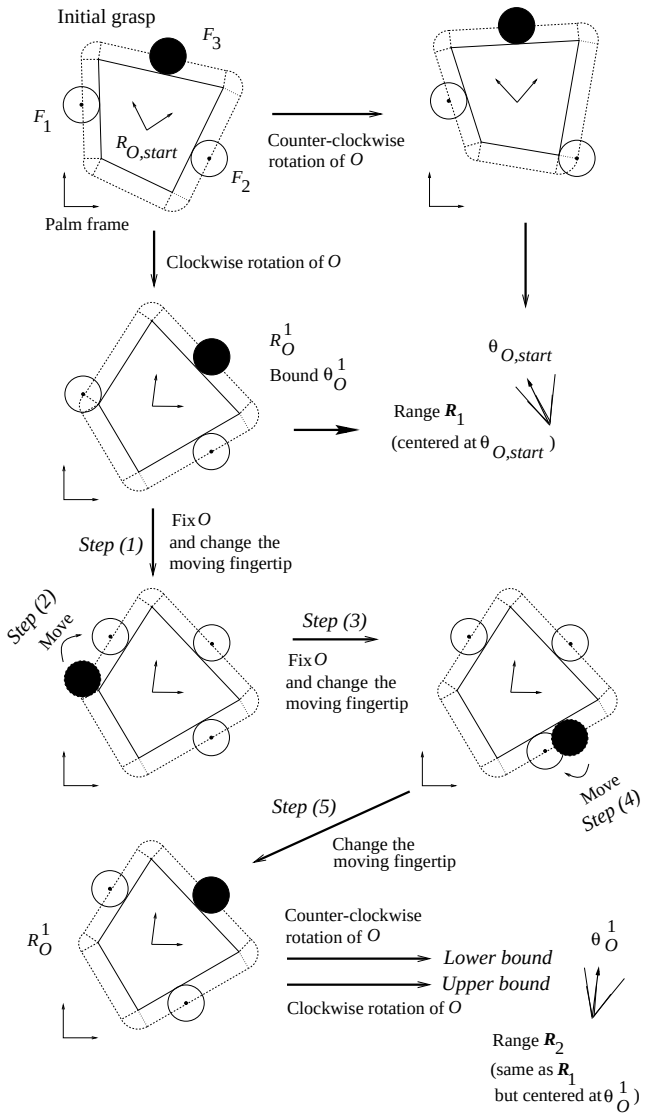

Figure 4: A 2-D case. Top left: the initial grasp of a polygon with 1 moving and 2 fixed fingertips. Second row: the resulting range $\mathcal{R}_1$ corresponding to the boundary orientations (top right and left second row). Third row and bottom left: re-grasping O. Bottom right: the resulting range $\mathcal{R}_2$ from the new grasp. The moved fingertip is shown in black and the fixed ones are white.

basic idea for enlarging the orientation range of O and obtaining $\mathcal{R}_2$ is as follows: *(1) fix O at an orientation, R_O^1, located close to one of the boundary of $\mathcal{R}_1$ (for instance the lower bound corresponding to clockwise rotation), fix the moving fingertip $F_{m=3}$ and select a fixed $F_i, i \in \{1,2\}$ to be moved, (let F_1 be this fingertip), (2) fix O and move F_1 towards its initial contact position $(u_{1,O}, v_{1,O})$, (3) fix O and F_1, (4) move F_2 towards its initial contact position $(u_{2,O}, v_{2,O})$, and (5) fix F_2 and consider $F_{m=3}$ as the moving fingertip* (see bottom Fig. 4). Notice that at the end of step (5), the grasp has changed *w.r.t.* $\mathcal{F}_P$, but has the same set of fixed fingertips and corresponding contact positions on O. Hence, the system (1) which is written *w.r.t.* $\mathcal{F}_O$ is exactly the same as for the initial grasp $\mathbf{g}_{start}$ and the resulting range $\mathcal{R}_2$ has the same structure as $\mathcal{R}_1$ (i.e., an open interval), but centered at R_O^1. Let R_O^2 be the new lower bound of $\mathcal{R}_2$. Processing the same above scheme, when starting from R_O^2, yields a third range $\mathcal{R}_3$. In order to cover entirely the interval $]-\pi, \pi]$, we re-iterate the same scheme in the neighborhood of each singular grasp. The idea being to add a range of motion having the same structure as $\mathcal{R}_1$ at each orientation close to a singularity. Notice that the $\mathcal{R}_j$'s overlap and that their union is $]-\pi, \pi]$. Therefore, the collection of corresponding S_j also cover $SO(2)$.

The construction of the ranges $\mathcal{R}_j$ in the 3-D case is processed similarly. Let n_1, n_2, and n_3 be the number of edges of the faces in contact with the fixed F_i's, respectively. Starting from $\mathbf{g}_{start}$, the resulting range $\mathcal{R}_1$ can be characterized by $n_1 + n_2 + n_3$ inequalities, each of them defining the constraint that a contact point must lie on one side of an edge. As we consider only convex polyhedra, $\mathcal{R}_1$ is in general a regular set[1]. The boundary of the closure set of $\mathcal{R}_1$ are orientations corresponding to (singular) grasps where at least a fingertip is on an edge or a vertex of O. As in the 2-D case, the basic idea consists in applying the above-described scheme to the 4 fingertips. This results in iteratively adding, at each orientation located close to the boundary of $\mathcal{R}_1$, a range of motion having the same structure $\mathcal{R}_1$ and centered at that orientation.

Because the geometry of $\mathcal{R}_1$ may be non-trivial, we illustrate our construction scheme using a simple spherical structure. The idea is to consider for building the $\mathcal{R}_j$'s a covering by spheres. The top left of Fig. 5 depicts the projection of an arbitrary range $\mathcal{R}_1$ on the plane (y, z). Let D be the larger sphere inscribed in $\mathcal{R}_1$ (top right of the figure). Building $\mathcal{R}_2$ consists in growing $\mathcal{R}_1$ by a distance equal to the radius of D (top right). The bottom left of Fig. 5 shows the projection on (θ_y, θ_z) of the resulting boundary of $\mathcal{R}_2$. The boundary of $\mathcal{R}_2$ is composed of a set of singular orientations that are processed as above (and at which a sphere D can be placed). Adding the spheres D's along the boundary of $\mathcal{R}_2$ yields enlarging the range of orientations of O (and obtaining $\mathcal{R}_3$). In the general case, one can start growing the 3-D structure of $\mathcal{R}_1$ by the spheres D until the full orientation space is covered. The boundaries of the resulting $\mathcal{R}_j$'s look like waves surrounding $\mathcal{R}_1$ at a distance $(j-1)R_D$, where R_D is the radius of D. Notice that the covering can be made finite by lower-bounding the distance between two adjacent spheres used for building a given range $\mathcal{R}_j$.

[1] Notice that $\mathcal{R}_1$ may be disconnected when the orientations of O are close to the boundary of the yaw/pitch/roll parameterization angles.

The idea of using the spheres D for incrementally covering the orientation space can be applied to show that each object orientation can be reached from the initial grasp in a finite time. Let $\theta_{O,goal}$ be any arbitrary orientation, and let $\mathcal{P}$ be the straight-line path connecting $\theta_{O,start}$ to $\theta_{O,goal}$ in the orientation space (see Fig. 6). $\mathcal{P}$ can be made feasible by covering it by a set of spheres D as shown in Fig. 6. Each D correspond to a different range $\mathcal{R}_j$. If the length of $\mathcal{P}$ is $l_{\mathcal{P}}$, a maximum of $\lceil l_{\mathcal{P}}/R_D \rceil + 1$ spheres are needed and re-orienting O can be achieved by the previous re-location scheme of the fixed fingertips in less of $\lceil l_{\mathcal{P}}/R_D \rceil + 1$ times. Because re-locating the fixed fingertips takes an upper-bounded time, the whole execution of $\mathcal{P}$ is finite.

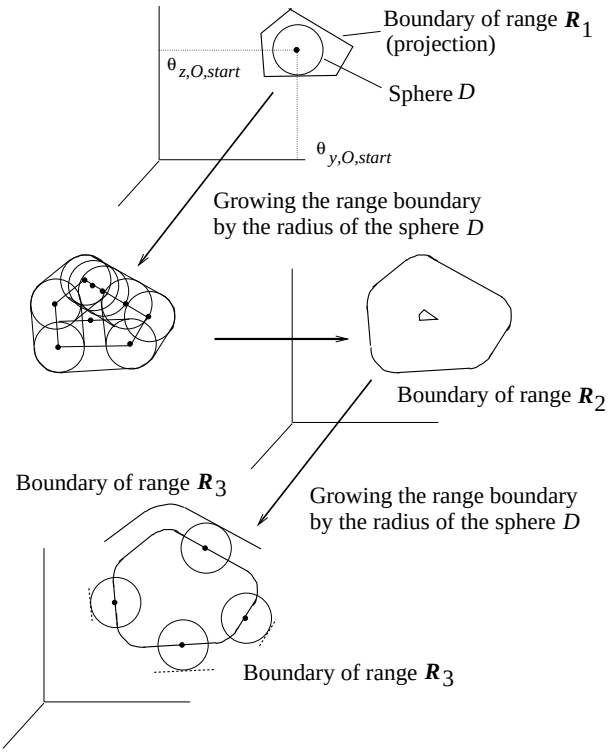

Figure 5: A 3-D case. Top left: the projection of the range $\mathcal{R}_1$ on the axes of rotations along z and y. initial grasp of a polygon. Top right: the maximum sphere D and growing $\mathcal{R}_1$ by the radius of D. Bottom: the resulting ranges $\mathcal{R}_2$ (left) and $\mathcal{R}_3$ (right).

4.2 Case of a convex smooth object

In the following, we derive an analysis enabling to show a conjecture that under some conditions (presented later), the C-space $CS_O(d)$, $d = 2, 3$, of a convex smooth object in

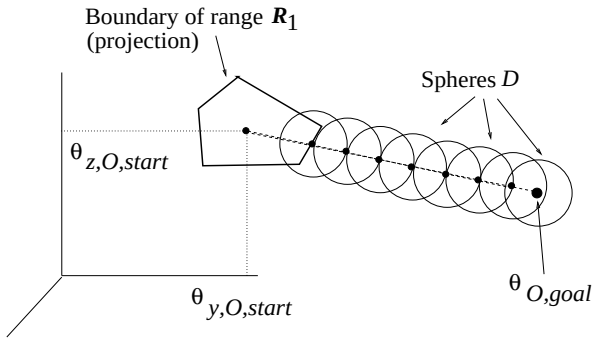

Figure 6: Transforming a path into a feasible motion using spherical covering.

contact with three fixed spherical fingertips is also globally diffeomorphic to $SO(d)$. For a convex smooth object, $CS_O(d)$ is a subset of $SE(d)$ defined by $\{g = (r_O, R_O) \in SE(d)/R_O \in SO(d)$ *and there exists a contact at each of the d fixed fingertips* $\}$. Since O is smooth, ∂O is a two dimensional manifold defined by a smooth function s. s is of the form $s(x, y, z, r_O, R_O) = 0$ and depends on the current configuration g_O, of O. As in §4.1, we enlarge O by the radii, ρ_i, of the F_i's as depicted in the 2-D case in Fig. 7.

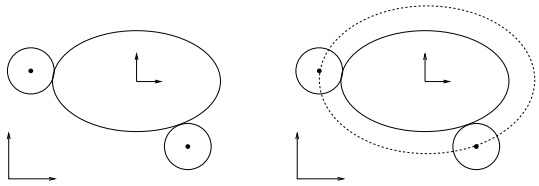

Figure 7: A 2-D case: an ellipse in contact with two fingertips.

Let $d = 3$ and let s' be the function parameterizing the surface resulting from enlarging O. Since O is smooth, s' is smooth. The conditions that the positions r_{F_i} of the fixed F_i's are on this surface are written $(w.r.t.\ \mathcal{F}_P)$

$$s'(x_{F_i}, y_{F_i}, z_{F_i}, r_O, R_O, \rho_i) = 0,\ i = 1 \ldots 3 \tag{2}$$

For a given orientation R_O and a given set of positions r_{F_i}, (2) defines a system of 3 nonlinear equations where the unknowns correspond to the components of r_O. This system may have no roots or several ones. In addition, it has no analytic solution in general, and only a numerical solution can be computed using an iterative method. When the convergence condition is satisfied in a neighborhood V of a root (e.g., the Jacobian of (2) is non singular or its spectral radius is strictly inferior to 1 [28, 36]), that root can be reached from any initial estimation lying in V.

For convex objects, hence convex functions s', the roots of (2) when they exist are two disjoint points (this will be explained later) or a single point. This means that one can define a neighborhood V containing only a single root and converge toward it using a numerical

method. Notice that we are only interested in the existence of the roots of (2) and their convergence neighborhoods. (Our goal is not to characterize them numerically). Because of the possible existence of multiple solutions, one cannot define a bijective map as in §4.1 with r_O being *the* solution of (2). However, starting from a current initial feasible grasp $\mathbf{g}^0$, one can consider only the closest root (if it exists) to r_O^0. For any orientation θ_O (parameterizing R_O) in a neighborhood $\mathcal{R}$ of θ_O^0, if (2) has at least a solution r_O and if r_O is chosen to be the closest root to r_O^0, we can define a bijection h between $\mathcal{R}$ and $I\!R^3 \times \mathcal{R}$. Since s' is differentiable, h is also differentiable and of full (column) rank. Applying the inverse function theorem (as in §4.1), it can be shown that h is a local diffeomorphism from $\mathcal{R}$ to $I\!R^3 \times \mathcal{R}$.

In the following, we illustrate our development in the case of an ellipsoid. Let $\rho_{O,x}$, $\rho_{O,y}$, and $\rho_{O,z}$ be the radii of O along the x, y, and z axes, respectively. The system of constraints (2) reduces to the form:

$$\frac{X_i^2}{(\rho_{O,x}+\rho_i)^2} + \frac{Y_i^2}{(\rho_{O,y}+\rho_i)^2} + \frac{Z_i^2}{(\rho_{O,z}+\rho_i)^2} - 1 = 0 \ , \ i = 1 \ldots 3 \tag{3}$$

where X_i, Y_i, and Z_i are the components of the vector $R_O^{-1} r_{F_i} - R_O^{-1} r_O$, ρ_i is the radius of F_i, and $\rho_{O,t}, t = x, y, z$ is the radius of O along the t-axis. Each nonlinear equation i in (3) constrains r_O to lie in a range defined by an ellipsoid E_i having the same shape as the enlarged object and centered at F_i. Fig. 8 depicts the ranges E_i for three fixed F_i. Note that all the E_i's have the same orientation R_O. (3) has a solution if the E_i's intersect at at least a point r_O. In addition, when (3) is solvable, at most 2 solutions may exist as illustrated by Fig. 9. In the following, we discuss the two cases:

1. When (3) has two disjoint roots, $r_{O,1}$ and $r_{O,2}$, as in Fig. 9, it is possible to find a neighborhood $\mathcal{R}$ of θ_O and a corresponding range V in $I\!R^3$ containing either $r_{O,1}$ or $r_{O,2}$ such that for each orientation in $\mathcal{R}$, (3) is well-defined and solvable and it has only one solution r_O in V. V correspond to the neighborhood of one of the two roots shown by the intersection of the closed curve $E_1 \cap E_2$ and the surface E_3 (see Fig. 9). This conjecture yields building a bijective map h which is a diffeomorphism between $\mathcal{R}$ and $V \times \mathcal{R}$.

2. When (3) has a single root at θ_O, it may happen that, for small displacements of O (hence of the E_i's) in some directions, the root vanishes. Our conjecture is that no neighborhood can be found around θ_O in which (3) is solvable at all orientations. When (3) is not solvable, this means that a contact is broken at one of the fixed fingertips. Therefore, the map h cannot be defined and the local diffeomorphism does not exist. The grasps corresponding to such situations are considered to be singular.

As for the case of polyhedral objects, avoiding singular grasps is tackled by applying the scheme defined previously (i.e., fixing O and selecting moving the fixed fingertips to their initial contact positions on O). The goal is to obtain a grasp deriving the same constrain system as the initial grasp. This permits enlarging the set of orientations reachable from the

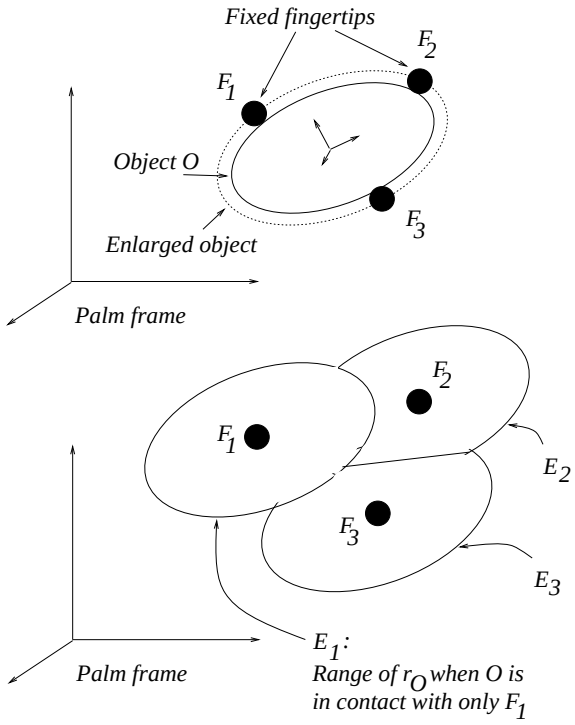

Figure 8: Ranges of motion of the center of an ellipsoid when it is in contact with 3 spherical fingertips. Each range correspond to the enlarged ellipsoid centered at a fingertip.

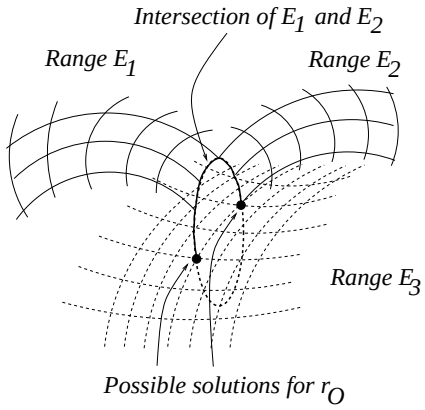

Figure 9: Two possible solutions for r_O. The closed curve is the intersection of E_1 and E_2 and correspond to the range of r_O where the object is in contact with only F_1 and F_2. Intersecting this curve with E_3 (i.e., adding the 3rd constraint of contact with F_3) gives two intersection points: the roots of (3). Notice that for some orientation, this intersection tends to be a single point.

singular grasps by the same range $\mathcal{R}$ (used for the initial grasp). Using the same sequential construction of the covering ranges performed for the polyhedron case, it can be show in a similar way that $SO(3)$ is globally diffeomorphic to $CS_O(3)$.

5 Overview of the planner

We now present a brief overview of our planning algorithm. The high level operates as a heuristic (A^* type) graph search on a discretized representation of a parameterization of $SO(3)$ (since CS_O is diffeomorphic to $SO(3)$). Starting from the initial grasp, it iteratively expands a tree, $\mathcal{G}$, of sub-goals (orientation cells). The expansion of $\mathcal{G}$ starts from $R_{O,start}$ and interleaves sequentially the following steps: (1) a set of sub-goal, $R_{O,g}$, is computed. It corresponds to the fact that O can be moved along a nominal path (corresponding to a pure rotation with an extreme velocity $\omega_{O,g}$ for a period of time ΔT). These new sub-goals are considered as new nodes in $\mathcal{G}$. (2) Starting from the current grasp, $\mathbf{g}_s$, a local planner is applied to find a (piece-wise) smooth feasible local trajectory segment satisfying the task constraints that moves the full manipulation system to a grasp $\mathbf{g}_g$ holding O at a sub-goal $R_{O,g}$ (or at an orientation within the same cell). (3) If such a trajectory segment is found, new sub-goals are generated from the reached orientation in unvisited adjacent nodes of $\mathcal{G}$, otherwise a local failure is reported and $R_{O,g}$ is considered to be non-reachable. These three steps are interleaved until a grasp holding O at its goal orientation, $R_{O,goal}$, is reached by the local planner (success), or no sub-goal can be reached locally during the search (failure).

In step (2), $R_{O,g}$ is selected to be the sub-goal which is located on the shortest path in $\mathcal{G}$. The computation of the length of the paths of $\mathcal{G}$ (including the heuristic term for evaluating the distance between $R_{O,g}$ and $R_{O,goal}$) is based on the following distance. For two arbitrary orientations $\theta_{O,1}$ and $\theta_{O,2}$, this distance is given by: $d(g_{O,1}, g_{O,2}) = \|\theta_{O,1,2}\|_2$, where $\theta_{O,1,2}$ is the orientation vector parameterizing the matrix $R(\theta_{O,1,2}) = R_O^T(\theta_{O,1})R_O(\theta_{O,2})$.

The local planner considers a local version of the re-orientation problem stated above where the end-points of the searched trajectory segment are the grasp $\mathbf{g}_s$ previously reached and the the current sub-goal, $R_{O,g}$. It makes use of the nominal velocity, $\omega_{O,g}$, used at the high level in order to guide the local search. This search operates iteratively at a finer increment of time, $\delta t << \Delta T$ and solves, at each instant δt, a linearized version of the quasi-static inverse motion problem to determine the contact forces while using the finger tracking strategy.

Instantaneous quasi-static motion prediction with friction and sliding constraints is often posed as a non-linear program (as shown by Trinkle for the forward problem when applying Peshkin's Minimum Power Principle (MPP) [30] and by Chong et al. for the inverse problem [7]). We derive and solve a linearized scheme, with the known nominal velocity, $\omega_{O,g}$, of O and by specifying (chosen in a random manner) explicitly the relative velocities at the contact points between the moving fingertip and O (we call these relative controls). This scheme decouples the problem of determining the new grasp and the problem of solving for contact forces. The application of the inverse solution to finger tracking is as follows:

1. Choose randomly one F_i to be moved and a relative control at its contact.
2. Determine a feasible rotation velocity that moves O toward its sub-goal, and compute its new configuration, $g_O(t + \delta t)$, resulting from displacing it for the period δt.
3. Knowing the configurations of the fixed F_i's and the velocity applied on O, determine for these fingertips the vector of relative controls at their contacts.
4. Knowing the relative controls at all the F_i's and the current grasp $\mathbf{g}(t)$ (hence, the current contact configuration), integrate Montana's contact kinematic equations [18] for the period δt. This results in new contact configurations which are used to compute the new configuration, $g_{F_i}(t + \delta t)$, of the moving fingertip (hence the new grasp $\mathbf{g}(t + \delta t)$).
5. If $\mathbf{g}(t + \delta t)$ is collision-free and reachable (i.e., if the moving F_i is within its finite workspace), solve the linearized inverse problem to compute the contact forces (by linear programming).[2]

This scheme is iterated until the sub-goal $R_{O,g}$ is reached in its cell (in this case, the planned trajectory segment is reported to the high level) or the system is deemed in a local minimum located out of this cell (in this case, a failure is reported to the high level).

[2] Although our scheme does not provide necessarily *the solution* to the prediction problem, it gives a possible solution (or an approximation) that can be used by a lower-level controller.

6 Local planning of feasible manipulation trajectories

6.1 The Constraints

Let $\theta_{O,g}$ be the orientation of O parameterizing the best sub-goal $R_{O,g}$ selected by the high level and let $\mathbf{g}_s$ be the grasp from which $\theta_{O,g}$ has been generated in the graph $\mathcal{G}$ via a hypothetical rotational motion of velocity $\omega_{O,g}$. The aim of the local planner –routine `LocalReorientation()`– is to check if $\theta_{O,g}$ can be effectively reached from $\mathbf{g}_s$ while coping with the complete set of the manipulation constraints. If it succeeds, the local planner provides the components of the local (piece-wise) smooth trajectory Γ_g ; a trajectory $\gamma_{O,g}(t)$ for O ending in the same cuboid cell as $\theta_{O,g}$, a trajectory, $\gamma_{F_i,g}(t)$, for each fingertip, and the set of contact forces f_i of the F_i's achieving $\gamma_{O,g}(t)$, $t \in [0, t_c]$.

Three types of constraints are considered by the local planner; geometric constraints (no overlapping between the fingertips, and between the object and the fingertips), force constraints (including friction and equilibrium of grasps), and the velocity constraints (object and fingertip velocities, and contact kinematics).

6.1.1 Force constraints

These concern friction and equilibrium constraints. Let $(f_{i,x}, f_{i,y}, f_{i,z})^T$ be the components of the (uni-lateral) pushing force f_i applied by F_i on O (written *w.r.t.* $\mathcal{F}_{c_i,O}$). Assuming a Coulomb friction model, $f_i, i = 1 \ldots k$ is constrained by $f_{i,x}^2 + f_{i,y}^2 \leq \mu^2 f_{i,z}^2$ (cone friction constraint) and $f_{i,z} \leq 0$ (pusing constraint), where μ is the coefficient of friction at the contact point. For a rolling (without sliding) contact, the contact force obeys these two constraints (we call these FRF). For a sliding contact, $f_i s$ must lie in the plane defined by the contact normal and the translational relative control $v_{r,t}^i$ (given by its components $v_{r,x}^i$ and $v_{r,y}^i$), and it must be of the same sign as $v_{r,t}^i$. That is, $f_i.(n_i \times v_{r,t}^i) = 0$ and $f_i.v_{r,t}^i \geq 0$. The two above constraints are re-formulated in the form (we call it FSF):

$$\left\{ \begin{array}{lcl} f_{i,x} & = & \alpha^i v_{r,x}^i \\ f_{i,y} & = & \alpha^i v_{r,y}^i \\ \alpha^i |v_{r,t}^i| & = & -\mu f_{i,z} \\ f_{i,z} \leq 0 & & \end{array} \right. \tag{4}$$

where α^i is an arbitrary strictly positive integer.

In addition to friction constraints and because the quasi-static assumption, the net of the f_i's must balance, at each instant, the external wrench applied on O (i.e., the gravitational force in our case). The equilibrium condition is given by:

$$G \ [\ f_1^T, 0_3^T, \ldots, f_k^T, 0_3^T \ ]^T = [\ -f_{O,ext}^T, 0_3^T \ ]^T \tag{5}$$

where 0_3 is the null vector of $\mathbb{R}^3$ (and means that no torsion moment along the axes is applied since O and the F_i's are rigid), and $f_{O,ext}$ is the gravity force applied on O.

6.1.2 Manipulation velocity constraints

At each instant, the velocity of O, $\dot{q}_O = (v_O^T, \omega_O^T)^T$ (written) *w.r.t.* $\mathcal{F}_O$) and the k velocities of the F_i's, $\dot{q}_{F_i}$ (written *w.r.t.* $\mathcal{F}_{F_i}$) are related by the matrix form [27, 19]:

$$\dot{q}_r = G^T \dot{q}_O - B_{c,H} \dot{q}_F \tag{6}$$

where $\dot{q}_r = ({q_r^1}^T, \ldots, {q_r^k}^T)^T \in \mathbb{R}^{6k}$ is the vector of velocities of O relative to the F_i's. ($\dot{q}_r^i = (v_{r,x}^i, v_{r,y}^i, v_{r,z}^i, \omega_{r,x}^i, \omega_{r,y}^i, \omega_{r,z}^i)^T$ is called the vector of relative control). In (6), $G \in \mathbb{R}^{6\times 6k}$ is the grasp matrix, $\dot{q}_F$ is $(\dot{q}_{F_1}^T, \ldots, \dot{q}_{F_k}^T)^T$, and $B_{c.H} \in \mathbb{R}^{6k\times 6k}$ is a diagonal matrix encoding the transformations between frames $\mathcal{F}_{F_i}$ and $\mathcal{F}_{c_i,O}$. In the following, we use the symbol $\breve{}$ to distinguish between rows of a given matrix corresponding to the translation basis (x, y, z) and rows corresponding to the rotation about these axes. For G^T, G_s^T $(s = x, y, z)$ is a $k \times 6$ matrix composed of the s rows of G^T, each corresponding to one F_i. $G_{\breve{s}}$ is a $k \times 6$ matrix corresponding to $\breve{s}$ rows. Similarly, $(B_{c,H})_s$ (resp. $(B_{c,H})_{\breve{s}}$) refers to the $k \times 6k$ matrix composed of the k rows of $B_{c,H}$, each corresponding to the s (resp. $\breve{s}$) row of $B_{c,H}$.

Maintaining the k contacts

We are interested in k-fingertip grasps. That is, breaking contacts is not allowed. The system of the k resulting constraints is:

$$\begin{bmatrix} v_{r,z}^1 \\ \ldots \\ v_{r,z}^k \end{bmatrix} = G_z^T \ \dot{q}_O - (B_{c,H})_z \ \dot{q}_F = \begin{bmatrix} 0 \\ \ldots \\ 0 \end{bmatrix} \tag{7}$$

Fixing three fingertips

Rewriting the constraint (7) when accounting for the fact that $\dot{q}_{F_i} = 0$ for the 3 fixed F_i's yields

$$\begin{cases} G_{j,z}^T \ \dot{q}_O = \ G_{j,z}^T \ (v_O^T, \omega_O^T)^T \ = \ 0 \\ j = 1 \ldots k \text{ and } F_j \text{ is a fixed fingertip} \end{cases} \tag{8}$$

where $G_i \in \mathbb{R}^{6\times 6}$ is the i-th component of G (it corresponds to F_i and is composed of the $6(i-1)+1$ to the $6i$ columns of G). Equation (8) is a 3×6 linear system where the unknown is $\dot{q}_O \in \mathbb{R}^6$. When the velocity of O is known along 3 degrees of freedom, and when (8) is not degenerate (i.e., the constraints are independent), (8) has a unique solution. For instance, when ω_O is known and the resulting system (8) is non-degenerate, v_O is unique.

Contact mode constraints

The relative controls of rolling are $(\omega_{r,x}^i, \omega_{r,y}^i)$. Relative controls of sliding are $(v_{r,x}^i, v_{r,y}^i)$, and $\omega_{r,z}^i$ is the relative control of twisting (rotation around the surface normal). In Table 1, we present the contact kinematic constraints (and corresponding force model) for different modes that can possibly occur at the contacts. We have used the same definitions as in [14].

Pure rolling	$v^i_{r,x} = v^i_{r,y} = 0$ $v^i_{r,z} = 0$ $(\omega^i_{r,x}, \omega^i_{r,y}) \in I\!R^2$ $\omega^i_{r,z} = 0$ f_i obeys FRF
Pure sliding	$(v^i_{r,x}, v^i_{r,y}) \in I\!R^2 \backslash \{(0,0)\}$ $v^i_{r,z} = 0$ $\omega^i_{r,x} = \omega^i_{r,y} = \omega^i_{r,z} = 0$ f_i obeys FSF
Pure twisting	$v^i_{r,x} = v^i_{r,y} = 0$ $v^i_{r,z} = 0$ $\omega^i_{r,x} = \omega^i_{r,y} = 0$ $\omega^i_{r,z} \in I\!R$ f_i obeys FRF
Rolling without sliding	$v^i_{r,x} = v^i_{r,y} = 0$ $v^i_{r,z} = 0$ $(\omega^i_{r,x}, \omega^i_{r,y}, \omega^i_{r,z}) \in I\!R^3$ f_i obeys FRF
Sliding	$(v^i_{r,x}, v^i_{r,y}) \in I\!R^2 \backslash \{(0,0)\}$ $v^i_{r,z} = 0$ $(\omega^i_{r,x}, \omega^i_{r,y}, \omega^i_{r,z}) \in I\!R^3$ f_i obeys FSF

Table 1: Contact modes and forces. FRF (resp. FSF) stands for Frictional Rolling (resp. Sliding) Force.

Our primary simulation results in dextrous manipulation have shown that it is very difficult to achieve quasi-static motions balancing the gravity wrench by sliding four-fingertip grasps [4, 5]. This is because, each sliding contact force is constrained to be in a particular direction given by the sliding velocity (model FSF). Our observation matches the result about the difficulty of firmly grasping polyhedra with a low number (four) of frictionless fingers [17, 16] (in this case, contact forces are always along the direction of the surface normal). In addition, we have observed that manipulation is made often easier when two fingertips are constrained to roll on the object without sliding. This is because the range of FRF (Frictional Rolling Forces) is the entire friction cone. For enhancing the ability of our specific manipulation strategy to perform quasi-static manipulation, we constrain, at each instant, two fingertips (a fixed F_i and the moving one) to be *rolling without sliding.* In particular, we constrain the moving F_i to be purely rolling, and we allow twisting at the fixed rolling fingertip. In both cases, contact forces obeys the FRF model. For the other fixed fingertips, we do not impose any specific contact mode. Hence, their relative controls depend on the current velocity $\dot{q}_O$ of O and may be any combination of rolling, sliding, and twisting (i.e., any mode given in Table 1).

Velocity bounds

The assumption of quasi-static analysis requires that the manipulation system moves slowly. For ensuring the validity of such an assumption, we consider that the velocities of the fingertips-object system are of bounded magnitudes. Therefore, we constrain, at each instant, the magnitude of the object velocity $\dot{q}_O$ and the pure rolling controls of the moving fingertip to be be upper-bounded by arbitrary small positive velocities.

6.2 Planning local feasible trajectories

In the following, we describe the basic instantaneous steps used by the local planner, at each increment of time δt, to find feasible manipulation trajectory for achieving the subgoal orientation $\theta_{O,g}$.

6.2.1 Solving the constrained motion of O

Because, we have introduced the additional kinematic constraint of rolling a fixed fingertip, O might not remain on the nominal path provided by the high level. Let assume that the current orientation of O is $\theta_O(t)$ and let $\tilde{\omega}_O$ be the rotation velocity moving O *freely* between $\theta_O(t)$ and $\theta_{O,g}$ along the shortest linear path (in $SO(3)$). Notice that $\tilde{\omega}_O = \omega_{O,g}$ when $\theta_O = \theta_{O,s}$.

Knowing $\tilde{\omega}_O$, we first transform it into a feasible velocity, ω_O, allowing O to be moved in contact with the three fixed fingertips when rolling at one of them. Let F_t be this fingertip. Rolling O on F_t without sliding contributes new constraints coupling the components of v_O

and ω_O. Indeed, we have the system of 5 linear equations and 6 unknowns:

$$\left\{\begin{array}{l} v^1_{r,z} = G^T_{1,z}\ \dot{q}_O = \ G^T_{1,z}\ (v^T_O, \omega^T_O)^T \ = \ 0 \\ v^2_{r,z} = G^T_{2,z}\ \dot{q}_O = \ G^T_{2,z}\ (v^T_O, \omega^T_O)^T \ = \ 0 \\ v^3_{r,z} = G^T_{3,z}\ \dot{q}_O = \ G^T_{3,z}\ (v^T_O, \omega^T_O)^T \ = \ 0 \\ v^t_{r,z} = G^T_{t,x}\ \dot{q}_O = \ G^T_{t,z}\ (v^T_O, \omega^T_O)^T \ = \ 0 \\ v^t_{r,z} = G^T_{t,y}\ \dot{q}_O = \ G^T_{t,z}\ (v^T_O, \omega^T_O)^T \ = \ 0 \\ t \in \{1 \ldots 3\} \text{ is the fixed rolling fingertip} \end{array}\right. \tag{9}$$

where the first three constraints form the system (8) and the two other constraints encode the no sliding condition at F_t (as in Table 1). We apply a simple scheme to determine (v_O, ω_O). It is based on transforming (9) into a 5×5 linear system by fixing one of the components of ω_O. This component is chosen to be the one having the highest magnitude and is determined by comparing the components of $\tilde{\omega}_O$. In other words, we chose to reduce the distance between $\theta_O(t)$ and $\theta_{O,g}$ along the farthest degree of freedom of rotation. When the resulting system is non degenerate, there is a unique solution for (v_O, ω_O) along which O can be moved. When this system is degenerate, we chose another component of ω_O to fix and we solve for the remaining velocity terms. If all combination have been unsatisfactorily considered, we consider that there is no feasible motion for O in the presence of the constraints (9) and for the current choice of the set of fixed fingertips and the rolling F_t. In this case, we select randomly a new set of fixed fingertips and a new F_t, and we re-iterate the same process. When there is a feasible (v_O, ω_O), we solve for the new configuration, $g_O(t + \delta t)$, of O considering the increment δt.

6.2.2 Solving the new contact configurations η_i

This step starts by choosing (resp. computing) a relative control for the moving (resp. fixed) fingertip(s) as follows:

- For the moving fingertip F_m, we randomly generate an extremal pure rolling relative control vector $\dot{q}^m_r$ considering the following sets, respectively:

$$\left\{\begin{array}{l} (\omega^i_{r,x}, \omega^i_{r,y}) \in \{\omega^{min}_{r,x}, 0, \omega^{max}_{r,x}\} \times \{\omega^{min}_{r,y}, 0, \omega^{max}_{r,y}\} \\ v^i_{r,x} = v^i_{r,y} = v^i_{r,z} = \omega^i_{r,z} = 0 \end{array}\right. \tag{10}$$

  where $(\omega^{min}_{.,.}, \omega^{max}_{.,.})$ are arbitrary constant lower- and upper-bounds of the pure rolling controls, respectively (cf. §6.1.2).

- For each of the three fixed fingertips, the relative controls are computed by solving the corresponding part of the system (6) which is given by:

$$\dot{q}^i_r = G^T_i \dot{q}_O,\ i \in \{1 \ldots k\},\ i \neq m \tag{11}$$

  where $k = 4$. For the fixed rolling fingertip F_t, (11) provides the relative controls $(\omega^t_{r,x}, \omega^t_{r,y}, \omega^t_{r,z})$ for rolling and twisting motions (we have $v^i_{r,x} = v^i_{r,y} = v^i_{r,z} = 0$). For the two other fixed fingertips, it provides $(v^i_{r,x}, v^i_{r,y}, \omega^i_{r,x}, \omega^i_{r,y}, \omega^i_{r,z})$ (we have $v^i_{r,z} = 0$).

Knowing the current grasp (including the contact configuration $\eta_i, i = \ldots k$) and the resulting relative controls $\dot{q}_r^i$'s, the contact velocity $\dot{\eta}_i$ is given by the following system of kinematic equations (Montana equations) [18]):

$$\begin{cases} \dot{\eta}_{i,O} = M_{i,O}^{-1} K_i^{-1} \left(\begin{bmatrix} -\omega_{r,y}^i \\ \omega_{r,x}^i \end{bmatrix} - \tilde{K}_{i,F_i} \begin{bmatrix} v_{r,x}^i \\ v_{r,y}^i \end{bmatrix} \right) \\ \dot{\eta}_{i,F_i} = M_{i,F_i}^{-1} R_\psi K_i^{-1} \left(\begin{bmatrix} -\omega_{r,y}^i \\ \omega_{r,x}^i \end{bmatrix} + K_{i,O} \begin{bmatrix} v_{r,x}^i \\ v_{r,y}^i \end{bmatrix} \right) \\ \dot{\psi}_i = \omega_{r,z}^i + T_{i,O} M_{i,O} \dot{\eta}_{i,O} + T_{i,F_i} M_{i,F_i} \dot{\eta}_{i,F_i} \\ v_{r,z}^i = 0 \end{cases} \tag{12}$$

where the M's, the K's, and the T's are the metric, curvature, and torsion tensor forms computed on each body at the contact c_i, respectively, $K_i = (K_{i,O} + \tilde{K}_{i,F_i})$ is the relative curvature at contact c_i, $\tilde{K}_{i,F_i} = R_{\psi_i} K_{i,F_i} R_{\psi_i}$, and $R_{\psi_i} \in I\!R^{2\times 2}$ is a rotation matrix corresponding to ψ_i (see [13, 18] for more details). (12) holds if K_i is invertible, and the objects in contact are rigid and locally smooth. These assumptions are valid in our case except on the edges of a polyhedron. We have extended Montana's equations to coping with this specific singular case when the contact is pure rolling or pure sliding (see appendix A).

Knowing the surface parameterization of the ∂F_i's and ∂O, we compute for the contact points $c_{i,F_i}(t + \delta t)$ and $c_{i,O}(t + \delta t)$. For F_m, we use the relationship $R_O c_{m,O} + r_O = R_{F_m} c_{m,F_m} + r_{F_m}$ to compute the new configuration $g_{F_m}(t + \delta t)$. $g_{F_m}(t + \delta t)$ is afterwards checked for the geometric (no collision and reachability) constraints. The collision test consists first of detecting if F_m overlaps with a fixed F_i. If no collision is detected, and if some F_i's are piece-wise smooth (e.g., a hemi-sphere), the test also checks if a contact occur between O and the non-smooth parts of these F_i's. This test aims to ensure the condition of "invertible curvature" at the contact. Finally, if $\mathbf{g}(t+\delta t)$ is collision-free, we check if F_m lies within its arbitrary finite workspace. If $\mathbf{g}(t + \delta t)$ is collision-free and reachable, we compute the corresponding contact forces f_i.

6.2.3 Solving the contact forces f_i

Our solution for determining the f_i's is based on solving the following linear program (LP) (by applying the *simplex* algorithm):

$$
\left\{
\begin{array}{l}
\textit{Minimize}: \quad P_v = -\dot{q}_O \cdot (f_{O,ext} + G\ f') \\
\textit{subject to}: \\
\quad G \ \left[\ f_1^T, 0_3^T, \ldots, f_k^T, 0_3^T\ \right]^T = \left[\begin{array}{c} -f_{O,ext} \\ 0_3 \end{array}\right] \\
\textit{and} \\
\quad f_{i,z} \leq 0 \quad i = 1 \ldots k \\
\textit{and} \\
\quad \left\{
\begin{array}{l}
\text{FRF } \textit{for rolling contact } c_{i,\ i\in\{1,\ldots,k\}} \\
\quad \left\{
\begin{array}{l}
-\mu'\ f_{i,z} \leq f_{i,x} \leq \mu'\ f_{i,z} \\
-\mu'\ f_{i,z} \leq f_{i,y} \leq \mu'\ f_{i,z}
\end{array}
\right. \\
\textit{or} \\
\text{FSF } \textit{for sliding contact } c_{i,\ i\in\{1,\ldots,k\}} \\
\quad \left\{
\begin{array}{lcl}
f_{i,x} & = & \alpha^i v^i_{r,x} \\
f_{i,y} & = & \alpha^i v^i_{r,y} \\
\alpha^i |v^i_{r,t}| & = & -\mu f_{i,z} \\
\alpha^i & \geq & 0
\end{array}
\right.
\end{array}
\right.
\end{array}
\right. \tag{13}
$$

where P_v corresponds to the instantaneous power of the manipulation system [24], and $f' \in I\!R^{24}$ is a vector defined by $(f_{1,x}, f_{1,y}, 0_4^T, f_{2,x}, f_{2,y}, 0_4^T, \ldots, f_{4,x}, f_{4,y}, 0_4^T)^T$, where 0_4 is the zero vector of $I\!R^4$. According to Peshkin [24], the forces involved in P_v are composed of all forces acting on O except forces of constraints (i.e., normal forces $f_{i,z}$). The constraints in (13) are equilibrium of O (i.e., the f_i's balance the gravity force, $f_{O,ext}$, applied on O), uni-laterality of the f_i's (i.e., the $f_{i,z}$'s push O along the opposite direction to the object outward normals), and friction constraints which are linearized depending on the type of motion (pure rolling for F_m, rolling without sliding for F_t, and any contact mode shown in Table 1 for the other fixed fingertips).

In the case of rolling, friction constraints have been simplified by approximating the friction cone by a 4-sides inscribed pyramid. $\mu' < \mu$ is the new friction coefficient obtained by this approximation. For a sliding contact and knowing the relative sliding velocity (cf. §6.2.2), the friction constraint is linearized. This is done by relating $f_{i,x}$ and $f_{i,y}$ with a variable $\alpha^i \geq 0$ which is considered as a new unknown in (LP).

6.2.4 The local algorithm

Starting from $\theta_{O,s}$, the local planner uses the three above-described steps as detailed in the following routine `LocalReOrientation`.

algorithm `LocalReOrientation`($\mathbf{g}_s, \theta_{O,g}, \omega_{O,g}$)
  $t_c = 0$;
  $\mathbf{g} = \mathbf{g}_s$;
  Choose randomly the fingertips F_m and F_t;
  Generate randomly the relative control $\dot{q}_m$ of F_m (cf. §6.2.2);

```
1   while ((θ_{o,g} not reached) & (bound_1()))
      { g_1 = g;     /* save the current grasp */
        compute ω̃_O;     /* when t = 0, ω̃_O = ω_{O,g} */
        feasible = TRUE;
        do
          {  if (¬ feasible)
               {  g = g_1;
                  Analyze the failure and choose randomly
                    a new F_m and/or a new F_t;
                  Generate randomly the control q̇_m;
                  Generate randomly ω_O among {0_3, ω̃_O};
                  feasible = TRUE; }
             if (ω_O ≠ 0_3)
               {  Transform ω_O into a feasible velocity and
                    determine v_O (cf. §6.2.1);
                  if (no feasible (v_O, ω_O) can be found)
                    {  feasible = FALSE;  goto 2;}
                  Compute the new configuration g_O(t_c + δt); }
             Compute the relative velocities at the fixed F_i's;
             Compute the new contact configurations (cf. §6.2.2);
             Compute the new configuration g_{F_m}(t_c + δt);
             Let g(t_c + δt) be the new grasp;
             if (collision at g(t_c + δt) or a contact is broken)
               {  feasible = FALSE;  goto 2;}
             if (g_{F_4}(t_c + δt) not reachable)
               {  feasible = FALSE;  goto 2;}
             Compute the contact forces f_i by solving (LP)
               given by (13) (cf. §6.2.3);
             if ((13) has no solution)
               feasible = FALSE;
2         } while ((¬ feasible) & (bound_2()));
        if (¬ feasible)
          {  g = g_1;  goto 2; }
        /* Γ_g is a sequence of grasps and contact forces */
        Γ_g = Γ_g ∪ {g(t_c + δt)} ∪ {f(t_c + δt)};
        t_c = t_c + δt;
      }
3   if (θ_O in the same cell as θ_{O,g})
      return(g,Γ_g,t_c);
    else
      return(∅);
  endalgorithm;
```

In the following, we detail some of the treatments in `LocalReOrientation`. We have used two different predicates `bound_1` and `bound_2` to ensure the termination of the local planner. The predicate `bound_1` is used to bound the duration t_c of the local trajectory

since O may be held stationary. `bound_2` bounds the number of trials applied when trying to escape a failure or a region of non feasible grasps. For instance, for the examples presented in this paper, `bound_1` corresponds to a limit of $2 * \Delta T$ and `bound_2` corresponds to a limit of 50.

A failure corresponds to violating one of the task constraints and it can be due to:

1. Collision between F_m and a fixed fingertip.
2. Non reachability of the resulting configuration of F_m.
3. Collision between O and the planar part of F_m when it is hemi-spherical.
4. Breaking a contact at one of the fixed fingertip when O is a polyhedron. This occurs when a fixed fingertip is close to an edge or a vertex.
5. Collision between O and the planar part of a fixed fingertip when it is hemi-spherical.
6. Gravity is not balanced by the contact forces.
7. Degeneracy of the system: this happens when the current grasp and the current set of fixed fingertips do not satisfy the non-degeneracy condition. No feasible velocity for O does exist for the resulting constraints. In this case, a fixed fingertip may have its contact broken or it can overlap with O.

When failures 1 and 3 occur, the guilty fingertip is F_m. In these two cases, we maintain the same F_m and we try to escape the failure by generating new relative controls to move it away from its previous position. Failure 4 is processed by moving the guilty fixed fingertip (enabling it to move between adjacent faces) and fixing the moving fingertip. Failures 5 to 7 are processed by selecting randomly a new F_m and a new F_t.

The local planner ends if the reached grasp $\mathbf{g}$ is deemed in a local minimum (i.e., no new grasp can be reached from it) or if the termination condition is satisfied. When the resulting object orientation is within the same cell as the sub-goal $\theta_{O,g}$, the local planner reports the trajectory and the contact forces to the high level. A new set of sub-goals are then generated in the search graph $\mathcal{G}$. Otherwise, it reports a failure and no expansion of the node $N(\theta_{O,s})$ is made.

7 Simulation results

We present simulation results carried out (on a Silicon Graphics Octane R10000 workstation, 175 MHz) for re-orienting convex polyhedra and convex smooth objects by four frictional fingertips F_i. More precisely, we consider the cases of a diamond-like object and an ellipsoid (a football). *These examples mainly bring out effects of our manipulation scheme and frictional contacts on the resulting trajectories of the manipulation system, and demonstrate the capacity of the scheme for achieving non-trivial re-orientation tasks.*

The fingertips are considered to be spherical. For a better illustration, we have considered different radii for the fingertips varying between 0.04 and 0.02 m. Notice that when the radii of the fingertips are different, the development we have presented in §4 remains valid (i.e., $SO(d), d = 2, 3$, is globally diffeomorphic to $CS_O(d)$). Each reachability region $\mathcal{W}_{F_i}$ of a fingertip is modeled by a sphere of radius equal to 0.1 (m). In the following examples, the considered mass of O is 1 Kg and the friction coefficient at each contact is $\mu_i = 0.7$.

In each of the following figures, the top left and the top middle snapshots show the initial grasp and the desired goal, respectively. The top right shows the final grasp (including the object orientation) achieved by the planner where the dark lines are the traces of the contacts on O. The middle of each figure shows a sequence of intermediate grasps achieved by the planner (i.e., elements of Γ). The bottom depicts the orientation path of O during the execution of Γ. The path is represented in the space of rotation along the x, y, and z axes of the fixed palm frame $\mathcal{F}_P$. The z axis is pointing upwards and the plane (shown by the rectangle) is the plane (x, y). The start and end orientations (end-points of of Γ) are shown on the right and on left side of the figures, respectively. For better illustration, we also project the orientation path on the plane (x, y). In each depicted grasp, the moving fingertip, F_m, is shown in solid black color, and the fixed rolling fingertip, F_t, is indicated in grey.

Tables 2 and 3 give the discretization used for processing the presented examples.

ΔT	δt	δ_θ (length cell)
2.0 s	0.1 s	2.406 deg.

Table 2: Time and configuration discretization.

$\omega_{O,x} = \omega_{O,y} = \omega_{O,z}$	$v_r^{min/max}$	$\omega_r^{min/max}$
1.43 deg./s	5 mm/s	2.86 deg./s

Table 3: Velocity discretization.

7.1 Case of a convex polyhedron

We have considered several different convex polyhedra. In the following, we present some re-orientation examples of a diamond-like polyhedron. The length of the diamond is about 0.35 m and the width is about 0.25 m. The considered initial and final orientations are (0.5, 0.4, 0.4) and (-0.5, -0.5, 0.7) (radian), respectively. Fig. 10 to 14 illustrate the planned trajectories for re-orienting the diamond considering four different scenario. The considered scenario are the following:

- Scenario D-1 (Fig. 10): At each instant, any fingertip can be selected to be moved. In addition, any fixed fingertip can be chosen to be rolling on O. F_m is allowed to move between any adjacent faces.

- Scenario D-2 (Fig. 12): The same as D-1 with the exception that F_m is not allowed to move between adjacent faces.
- Scenario D-3 (Fig. 13): The planner chooses, once in the beginning, F_t. F_t is maintained the same during the re-orientation task. F_m is selected, at each instant, among the three remaining fingertips, and is allowed to move between adjacent faces.
- Scenario D-4 (Fig. 14): The same as D-3 with the exception that F_m is not allowed to move between adjacent faces.

Table 4 gives the cpu-time and the cardinality of the sub-goals explored during the computation of the trajectories Γ.

Example	D-1	D-2	D-3	D-4
Nodes of $\mathcal{G}$	187	241	199	209
Sub-goals explored locally	42	131	70	54
Sub-goals $\in \Gamma$	35	43	41	41
cpu time (s)	53	107	89	82

Table 4: Solution parameters: case of a diamond-like polyhedron

Scenario D-1 (Fig. 10) corresponds to the most effective manipulation scheme since the planner can select any combination of fixed fingertips and F_m can move between adjacent faces. As we have pointed out §6.1.2, manipulation is very often performed through two rolling and two sliding contacts. The ability to change the set of fixed fingertips and the set of rolling ones (i.e., F_m and F_t) has its effect in increasing the capacity of the randomized instantaneous solution for two reasons: (1) it is easier to find a contact distribution to balance the gravity wrench and (2) the range of reachable orientations is enlarged since considering different combination of moving/fixed fingertips contributes increasing the number of performed grasps as it was partly illustrated in §4.1. In §4.1, changing the grasps and re-locating the F_i's on O were performed in the absence of the reachability constraints. When dealing with reachability constraints and for certain object motions, it becomes more difficult to maintain the moving fingertip F_m in its reachable workspace $\mathcal{W}_{F_m}$ without switching it between faces. This is illustrated in Fig. 11 where F_m must make a new contact with a new face in order to be able to safely perform the clockwise re-orientation of O and to perform a kinematically feasible (and safe) manipulation motion.

We have observed that applying scenario D-1 often yields object motions which are very close to the shortest path. Remember that we have used a distance (cf. §5) which is different from the usual Euclidean distance between the orientation parameters. If the latter distance is used, the shortest path corresponds to the straight-line connecting the two end-orientations. In our case, the shortest path is a more elaborate curve. As shown in Table 4, 42 sub-goals were explored locally in scenario D-1 and Γ goes through 35 of them. The

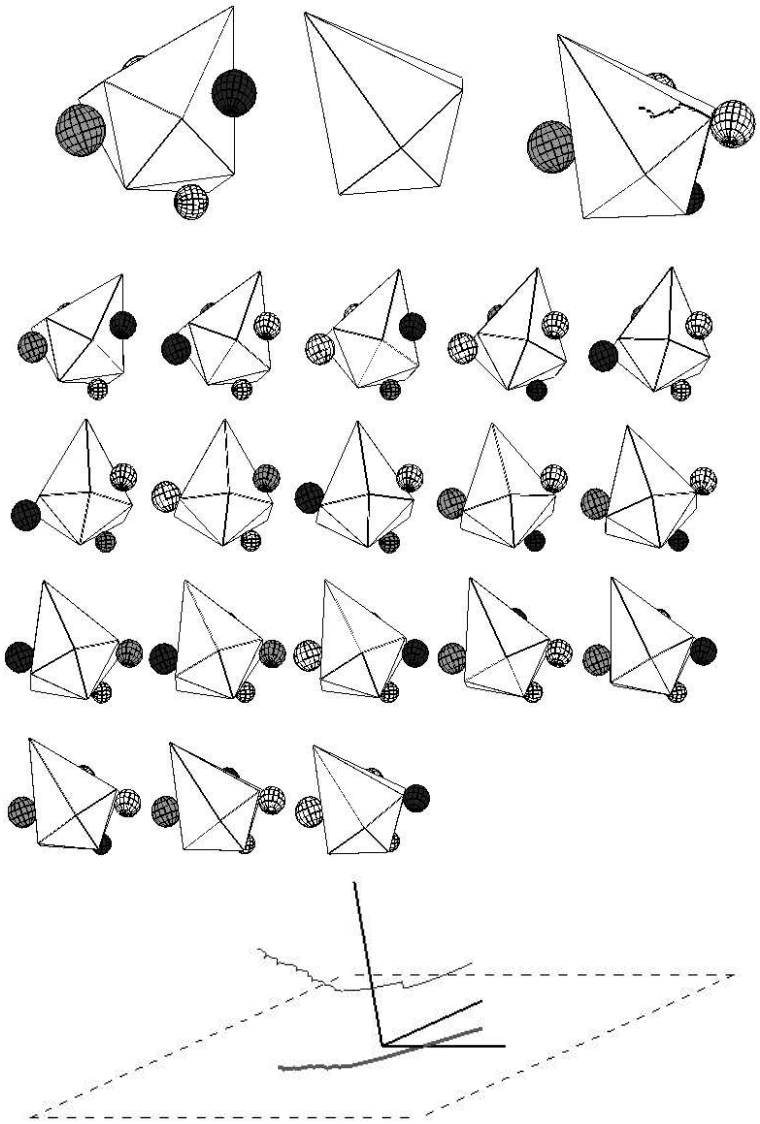

Figure 10: Scenario D-1 (bottom: z-axis is pointing upwards).

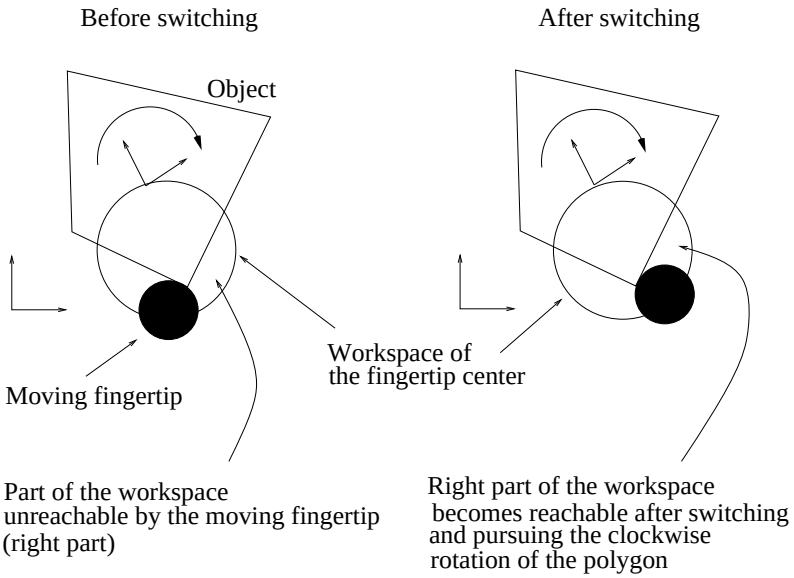

Figure 11: A 2-D illustration of enlarging the range of feasible safe and reachable grasps by switching the moving fingertip, F_m, between adjacent faces.

computation time required for planning is less than a minute. The performance of the planner changes drastically when F_m is not allowed to move between faces during manipulation (as in scenario D-2). Indeed, the planner takes almost twice the time needed for D-1. The local planner explores 131 sub-goals and Γ goes through 107 of them. Several maneuvering have been performed close to the orientation goal and correspond to orientations where F_m avoided the edges of O.

Scenario D-3 and D-4 are performed when the fixed rolling fingertip, F_t, is maintained the same during the task (see Fig. 13 and 14). The performance of the planner is shown in Table 4. The geometry of both trajectories in D-1 and D-3 are similar with the exception of a sudden vertical drop close to the middle of the trajectory. This corresponds to changing the moving fingertip F_m, which affects the range of feasible instantaneous object velocities (translation and rotation) since the governing kinematic equations (9) of the system changed. In D-2 and D-4, such a drop did not happen. We have also observed that many maneuvering were performed close to the end of Γ as indicated by the "oscillatory" nature of the trace of the orientation curve in Figs. 12 and 14 (particularly for D-2) (the end of Γ is shown on the left side of the figures). This is because avoiding breaking contacts and moving across the edges of O is non-trivial when the fixed fingertips are located close to the boundary of the object faces.

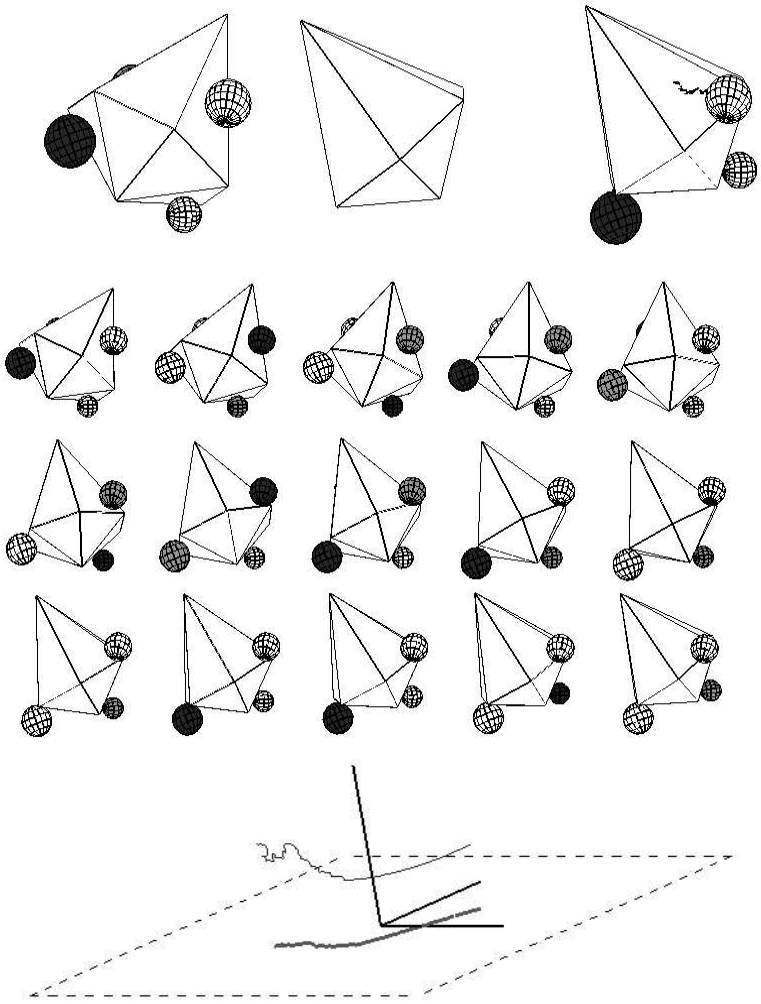

Figure 12: Scenario D-2 (bottom: z-axis is pointing upwards).

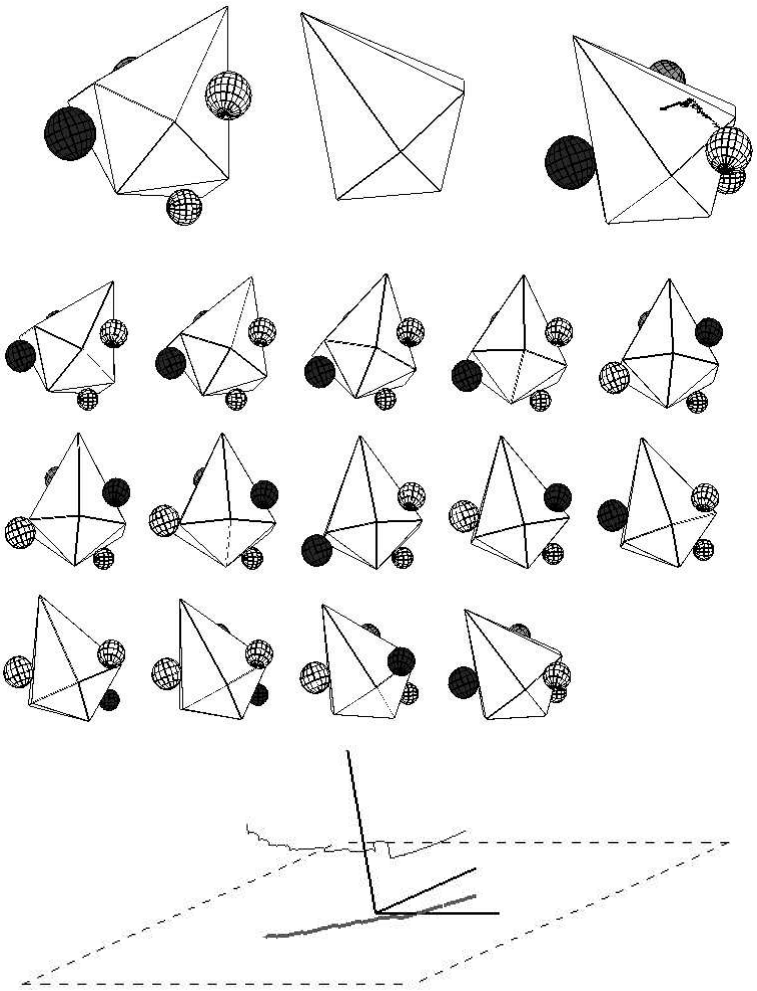

Figure 13: Scenario D-3 (bottom: z-axis is pointing upwards). The selected fingertip F_t is located at the back of the object O.

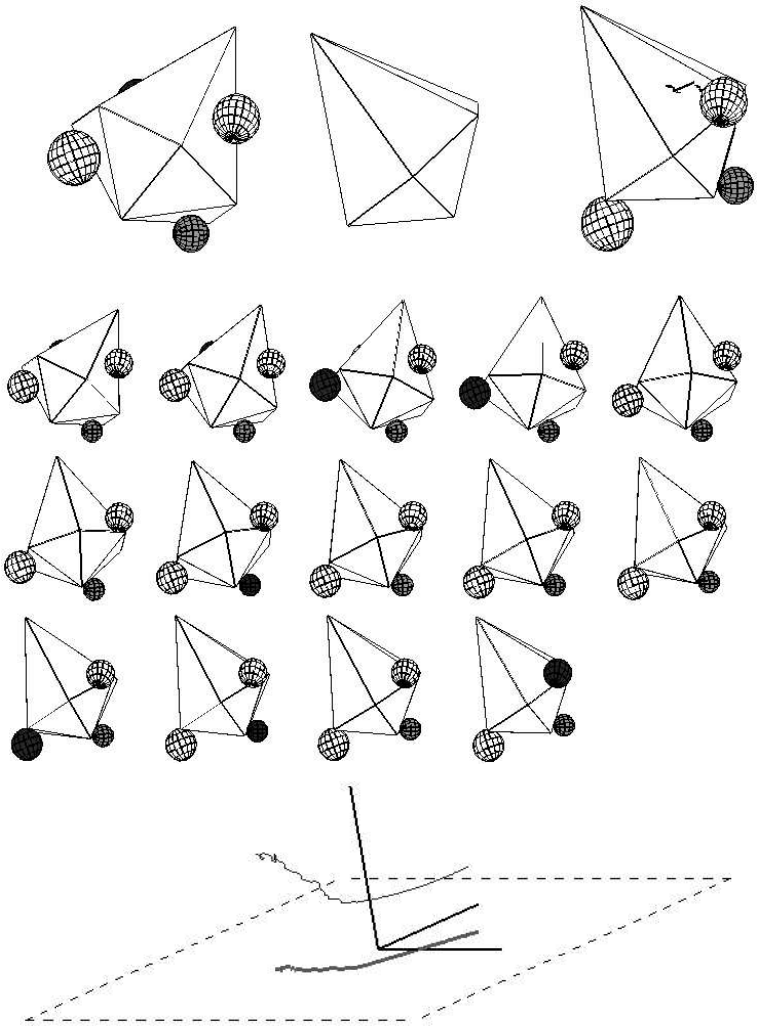

Figure 14: Scenario D-4 (bottom: z-axis is pointing upwards).

7.2 Case of a convex smooth object

In the following, we present some experiments showing the applicability of the planner to solve re-orientation tasks of a smooth object – for instance, a football-like ellipsoid – by 4 frictional hemi-spherical fingertips. The radii of the football along the x and y axes are equal to 0.09 m and the radius along the z axis is 0.12 m. The considered initial and final orientations are (0.5, 0.7, 0.4) and (-0.6, -0.5, 0.8) (radian), respectively.

We have considered two different scenario as follows:

- Scenario F-1 (Fig. 15): F_m and F_t are chosen randomly at each instant.
- Scenario F-2 (Fig. 16 to 18): F_m is randomly chosen at each instant while F_t is selected once in the beginning.

Table 5 gives the cpu-time and the cardinality of the sub-goals explored during the computation of the trajectories Γ. Scenario F-1 (like D-1) results in easy planning since Γ goes through all the sub-goals explored locally. The second scenario (when F_t is chosen once in the beginning) is depicted by the results of three executions of the planner (Fig. 16 to 18). The effect of the randomness of the planner is illustrated by the obvious difference between the three solutions.

Example	F-1	F-2.1	F-2.2	F-2.3
Nodes of $\mathcal{G}$	247	252	373	347
Sub-goals explored locally	44	50	252	216
Sub-goals $\in \Gamma$	44	49	74	75
cpu time (s)	43	118	183	119

Table 5: Solution parameters: case of a football

In Fig. 17 and 18, the same F_t is considered. Our conjecture is that because F_t is located near the top of O (above the center of mass of O), it is difficult to balance gravity and the sliding forces of the two other fixed fingertips with F_m and F_t. This explains the performance of the planner (locally explored sub-goals, length of Γ, and run time). When F_t is located below the center of mass (as in Fig. 16), it becomes easy to achieve equilibrium of O.

In summary, our simulation results are:

- It is easy for the planner to solve re-orientation tasks quickly when F_m and F_t can be changed at each instant.
- The planner has similar performance for both cases of polyhedra and smooth objects.
- In the case of polyhedra, the contact kinematics is simple (since the geometric forms in Montana's equations are constant) but moving F_m between adjacent faces must be performed accurately and continuously. This requires addition collision detection at each increment of time δt.

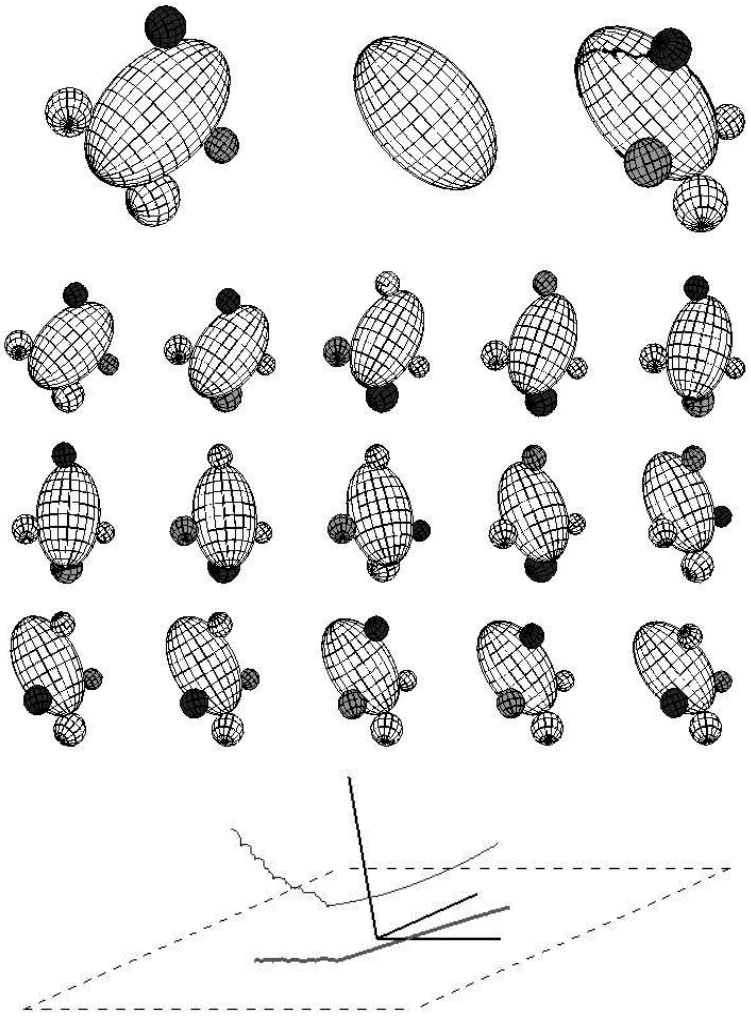

Figure 15: Scenario F-1 (bottom: z-axis is pointing upwards).

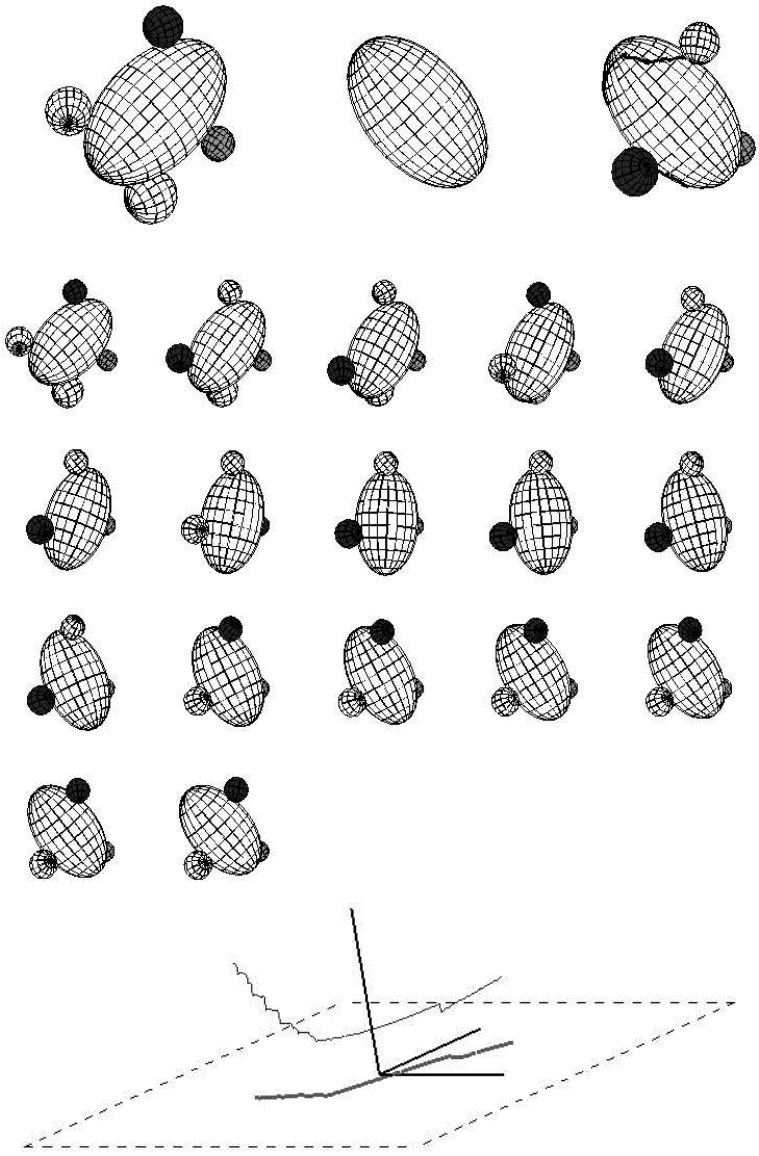

Figure 16: Scenario F-2.1 (bottom: z-axis is pointing upwards).

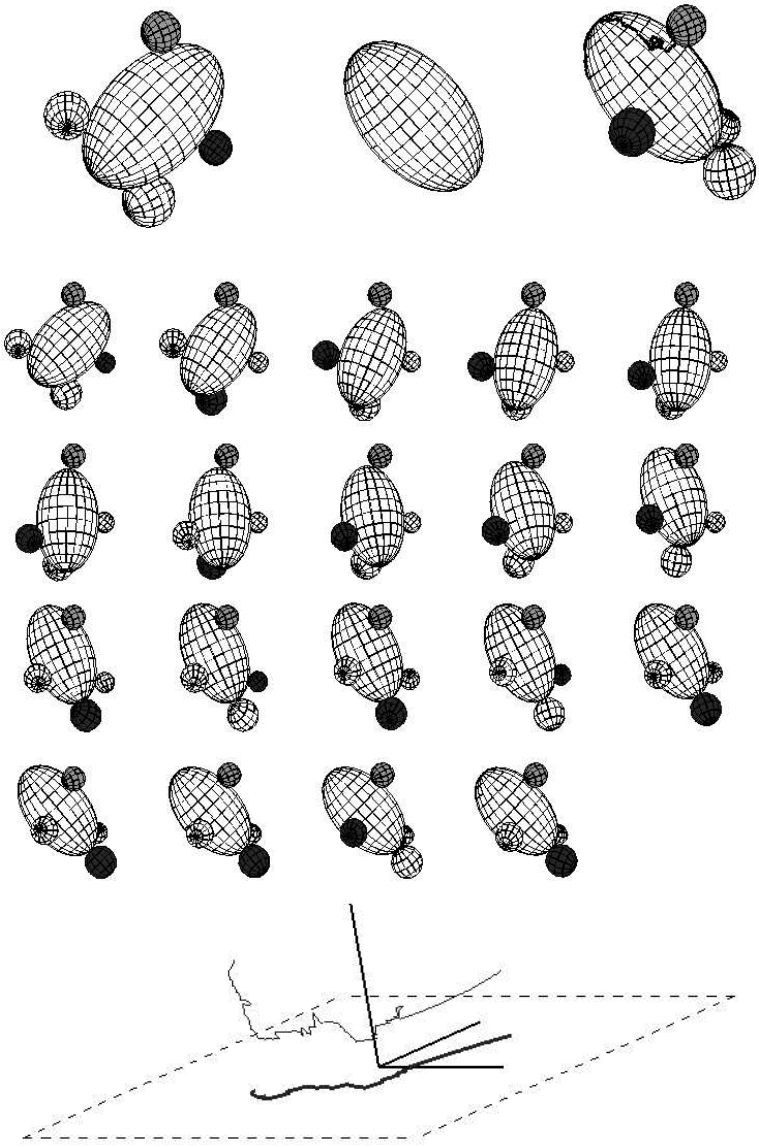

Figure 17: Scenario F-2.2 (bottom: z-axis is pointing upwards).

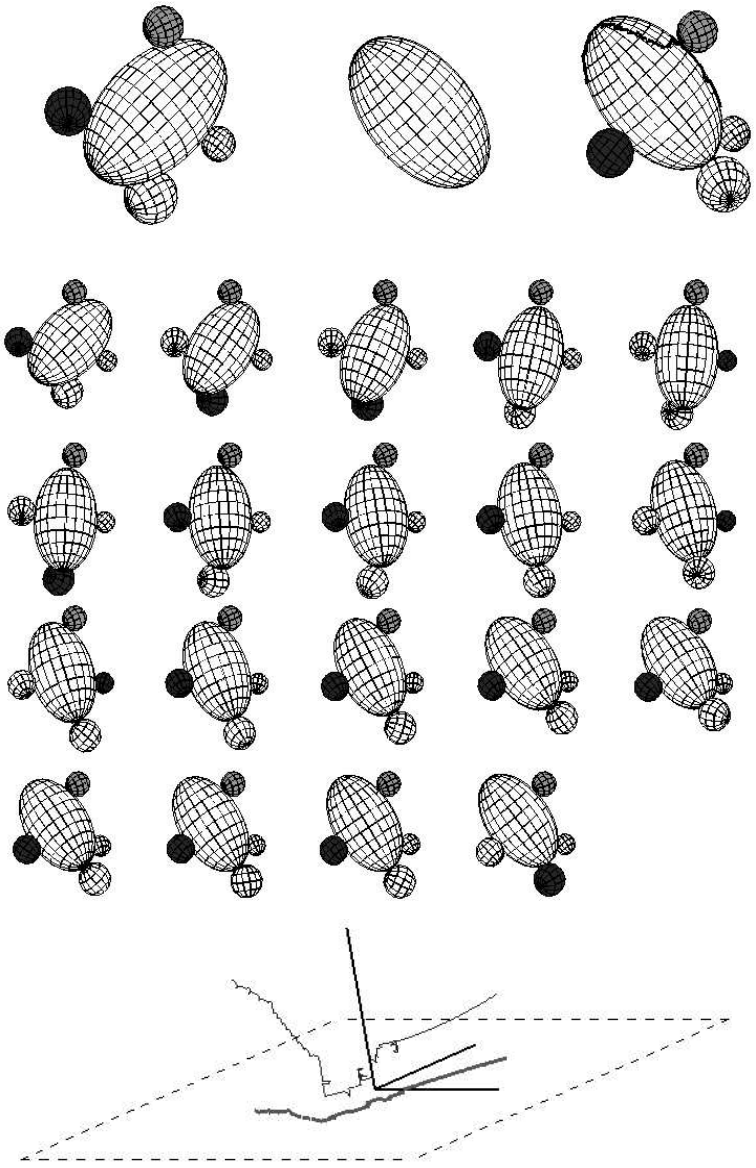

Figure 18: Scenario F-2.3 (bottom: z-axis is pointing upwards).

- In the case of smooth objects, the contact kinematics is more elaborate and the geometric forms in Montana's equations are not constant and must be re-computed at each δt.
- Because of the randomness of the local level, the planner may provide different solutions whose geometry can vary significantly for the same task.

8 Conclusion

In this paper, we have addressed the motion planning problem for global re-orientation of 3-D convex polyhedral and smooth objects by four-fingertip grasps. We concentrated on a particular scheme consisting of constraining the motion of the object by fixing, at each instant, three fingertips and acting on it by moving the fourth fingertip. The novelty of our work is in applying key ideas (for organizing and structuring the search for feasible trajectories) from gross motion planning that integrate and combine the "randomized finger tracking" strategy and different frictional contact modes for finding feasible motions and contact forces to achieve non-trivial 3-D re-orientation tasks automatically. Our two-level planning algorithm effectively deals with several aspects of (piecewise-) smooth dextrous manipulation that make it a difficult and challenging problem: high dimensionality of the C-space of the fingertip-object system, effect of friction and kinematics of the contacts on achieving quasi-static manipulations, collision avoidance and grasp reachability constraints. In particular, it exploits the constraints due to fixing three fingertips in order to reduce the dimension of the search space. The solution led to a practical implementation which has been applied successfully to several realistic frictional re-orientation tasks of polyhedral and smooth objects. The results demonstrated the power and promise of our planner.

The planner, as it is structured, can be extended to incorporate the finger chain kinematics as described in [6]. In addition, the planner can be applied to any effector composed of more than four fingertips. For three-fingertip grasps, the idea of reducing the search space can be conceptually applied when, for instance, two fingertips must be fixed at each instant.

The assumptions we made (e.g., rigid bodies, and perfect knowledge of the geometric and physical aspects of the system) and the manipulation modes we considered are reasonable as a first stab for global planning for dextrous manipulation. Indeed, the discrepancy between these models and the real tasks combined with the difficulty of controlling rolling and sliding motions may yield problems during the actual execution of the planned trajectories. While some of the above mentioned assumptions can be relaxed within our planning framework (particularly, soft contacts and model uncertainties), some others are related to sensing, mechanics and control issues, which are beyond the scope of this paper and merit further investigation in our future research.

References

[1] A. Bicchi. On the closure properties of robotic grasping. *IJRR*, 14(4):319–334, 1995.

[2] D. L. Brock. Enhancing the dexterity of a robot hand using controlled slip. In *IEEE ICRA*, pages 249–254, 1988.

[3] M. Cherif. Motion planning for all-terrain vehicles: A physical modeling approach for coping with dynamic and contact interaction constraints. *IEEE Trans. on Robotics & Automation*, 15(2):202–218, Apr. 1999.

[4] M. Cherif and K. K. Gupta. Planning quasi-static motions for re-configuring objects with a multi-fingered robotic hand. In *IEEE ICRA*, pages 986–991, Albuquerque (USA), Apr. 1997.

[5] M. Cherif and K. K. Gupta. Practical motion planning for dextrous re-orientation of polyhedra. In *IEEE/RSJ IROS*, pages 291–297, Grenoble (F), Sep. 1997.

[6] M. Cherif and K. K. Gupta. Planning for in-hand dextrous manipulation. In L. Kavraki P. Agarwal and M. Mason, editors, *Robotics, the Algorithmic Perspective*, pages 103–118. A.K. Peters Publisher, Wellesley (MA), USA, 1998.

[7] N. Y. Chong *et al.* A generalized motion/force planning strategy for multifingered hands using both rolling and sliding contacts. In *IEEE/RSJ IROS*, pages 113–120, 1993.

[8] A. B. Cole, J. E. Hauser, and S. S. Sastry. Kinematics and control of multifingered hands with rolling contact. *IEEE Trans. on Automatic Control*, 34(4):398–404, 1989.

[9] A. B. Cole, P. Hsu, and S. S. Sastry. Dynamic control of sliding by robot hands for regrasping. *IEEE Trans. on Automatic Control*, 8(1):42–52, 1992.

[10] R. S. Fearing. Simplified grasping and manipulation with dextrous robot hands. Technical Report, A.I. Memo 809, A.I. Lab. MIT, MA, 1984.

[11] R. S. Fearing. Implementing a force strategy for object re-orientation. In *IEEE ICRA*, pages 96–101, San Francisco (USA), 1986.

[12] K. K. Gupta. Motion planning for re-orientation using finger tracking: Landmarks in $so(3) \times \omega$. In *IEEE ICRA*, pages 446–451, Nagoya (J), 1995.

[13] Z. Li and J. Canny. Motion of two rigid bodies with rolling constraint. *IEEE Trans. on Robotics & Automation*, 6(1):62–72, 1990.

[14] Z. Li, J. Canny, and S. S. Sastry. On motion planning for dextrous manipulation, part I: the problem formulation. In *IEEE ICRA*, pages 775–780, Scottsdale, AZ (USA), 1989.

[15] Z. Li, P. Hsu, and S. S. Sastry. Grasping and coordinated manipulation by a multifingered robot hand. *IJRR*, 8(4):33–50, Aug. 1989.

[16] X. Markenscoff, L. Ni, and C. H. Papadimitriou. The geometry of grasping. *IJRR*, 9(1):61–74, 1989.

[17] B. Mishra, J. T. Schwartz, and M. Sharir. On the existence and synthesis of multifinger positive grips. *Algorithmica*, 2(4):541–558, 1987.

[18] D. J. Montana. The kinematics of contact and grasp. *IJRR*, 7(3):17–31, 1988.

[19] R. M. Murray, Z. Li, and S. S. Sastry. *A Mathematical Introduction to Robotics Manipulation*. CRC Press, 1994.

[20] V. Nguyen. Constructing force closure grasps. *IJRR*, 7(3):3–16, 1988.

[21] T. Omata and M. A. Farooqi. Regrasps by a multifingered hand based on primitives. In *IEEE ICRA*, pages 2774–2780, Minneapolis, MN (USA), Apr. 1996.

[22] T. Omata and N. Nagata. Planning reorientation of an object with a multifingered hand. In *IEEE ICRA*, pages 3104–3110, San Diego, CA (USA), May 1994.

[23] S. Payandah. Planning controlled slips in dextrous manipulation. In *IEEE ICRA*, Albuquerque (USA), 1997.

[24] M. A. Peshkin and A. C. Sanderson. Minimization of energy in quasi-static manipulation. *IEEE Trans. on Robotics & Automation*, 5(1):53–60, 1989.

[25] D. Rus. *Fine Manipulation Planning for Dextrous Manipulation*. PhD thesis, Dep. of Computer Science, Cornell University, 1992.

[26] D. Rus. In-hand dexterous manipulation of piecewise-smooth 3-d objects. *IJRR*, 18(4):355–381, Apr. 1999.

[27] K. Salisbury. *Kinematics and Force Analysis of Articulated hands*. PhD thesis, CS Dept., Stanford University, 1982.

[28] H. R. Schwarz. *Numerical Analysis, A comprehensive introduction*. John Wiley & Sons Ltd, 1989.

[29] K. B. Shimoga. Robot grasp synthesis algorithms: a survey. *IJRR*, 15(3):230–266, 1996.

[30] J. C. Trinkle. A quasi-static analysis of dextrerous manipulation with sliding and rolling contacts. In *IEEE ICRA*, pages 788–793, Scottsdale, AZ (USA), 1989.

[31] J. C. Trinkle and J. J. Hunter. A framework for planning dexterous manipulation. In *IEEE ICRA*, pages 1245–1251, Sacramento (USA), May 1991.

[32] J. C. Trinkle and R. Paul. Planning dextrous manipulation with sliding contacts. *IJRR*, pages 24–48, 1990.

[33] J. C. Trinkle and D. C. Zeng. Prediction of the quasistatic planar motion of a contacted rigid object. *IEEE Trans. on Robotics & Automation*, 11(2):229–246, 1995.

[34] J.C. Trinkle, A.O. Farahat, and P.F. Stiller. First-order stability cells of active multi-rigid-body systems. *IEEE Trans. on Robotics & Automation*, 11(4):545–557, 1995.

[35] J.C. Trinkle, S.L. Yeap, and L. Han. When quasistatic jamming is impossible. In *IEEE ICRA*, pages 3401–3406, Minneapolis (MN), Apr. 1996.

[36] E. E. Tyrtyshnikov. *A Brief Introduction to Numerical Analysis.* Birkhäuser, Boston, MA, 1997.

A Fingertip motion between adjacent faces

In this section, we report on the case when the manipulated object O is a polyhedron. Let ∂O_p and ∂O_q be two given adjacent faces of O, and e_{pq} be their intersecting edge. We present in the following how a transition motion of a fingertip F between ∂O_p and ∂O_q is processed during the computation of new grasps. Let $c_{O,1} = (u_{O,1}, v_{O,1})$ be the coordinates of the point of a contact c_o *w.r.t.* a fixed frame on ∂O_p, and let $c_{O,2} = (u_{O,2}, v_{O,2})$ be the new position obtained by solving Montana's equations. Note that $c_{O,2}$ lies on the same plane supporting ∂O_p. A transition motion between the two faces occurs when $c_{O,2}$ is outside the boundary of ∂O_p. In this case, the instantaneous re-location of F on ∂O_q is necessary to maintain contact. Hence a new position $c_{i,3} = (u_3, v_3)$ on ∂O_q of the contact has to determined together with the new position (u_F, v_F) of contact on the surface of F and the angle of contact ψ. The latter parameters depend on the contact mode, i.e., rolling or sliding.

Let p be the intersection point between e_{pq} and the direction of the Cartesian motion between $c_{O,1}$ and $c_{O,2}$, and u_{pq} be the unit vector of e_{pq} as depicted in Fig. 19. Note that locally, the parameters $(u_{O,3}, v_{O,3})$ are located on another chart than ∂O_p, and that p and u_{pq} can be written *w.r.t.* to both of these charts. The new position of $c_{O,3}$ is depicted on Fig. 19, and obtained by using the following relationships:

$$\begin{aligned} & \vec{pc}_{O,2/\mathcal{F}_q} = R(n_q, -\beta)\ u_{pq/\mathcal{F}_q} \\ & \cos\beta = \frac{\vec{c_{O,1}c}_{O,2/\mathcal{F}_p} \cdot u_{pq/\mathcal{F}_p}}{\|\vec{c_{O,1}c}_{O,2/\mathcal{F}_p}\|_2} \\ & \sin\beta \geq 0 \end{aligned} \tag{14}$$

where n_q is the normal to ∂O_q, and R is a rotation matrix about n_q.

The last treatment concerns the positions of contact on the surface of F and the angle of contact ψ. These positions depend on the current type of the contact mode. For both rolling and sliding motions, the new angle of contact ψ_3 is given by:

$$\psi_3 = \psi_2 + \arccos(x_p \ .\ R(u_{pq}, \pi - \phi_{pq}) x_q) \tag{15}$$

where ψ_2 is the contact angle obtained by solving (12), ϕ_{pq} is the angle between the two faces, and x_p and x_q are the x-axes of the frames $\mathcal{F}_p$ and $\mathcal{F}_q$ fixed on ∂O_p and ∂O_q, respectively.

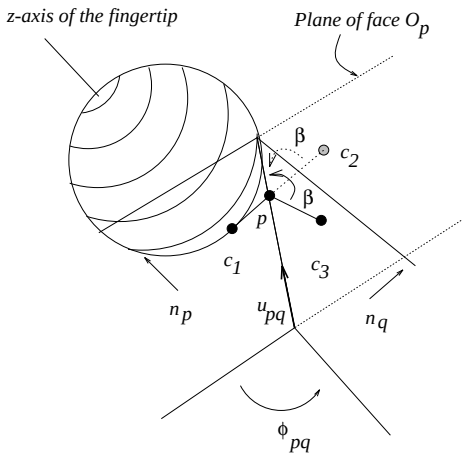

Figure 19: The new contact position after a transition motion on a polyhedral object.

When F is rolling, we have:

$$(u_{3,F}, v_{3,F}) = (u_{2,F}, v_{2,F}) \tag{16}$$

When F is sliding, its orientation is maintained constant *w.r.t.* the palm frame $\mathcal{F}_P$. Exploiting this and knowing the new position $c_{O,3}$ on ∂O_q, we can compute for that position *w.r.t.* $\mathcal{F}_F$ and deduce the parameters $(u_{3,F}, v_{3,F})$ on ∂F.

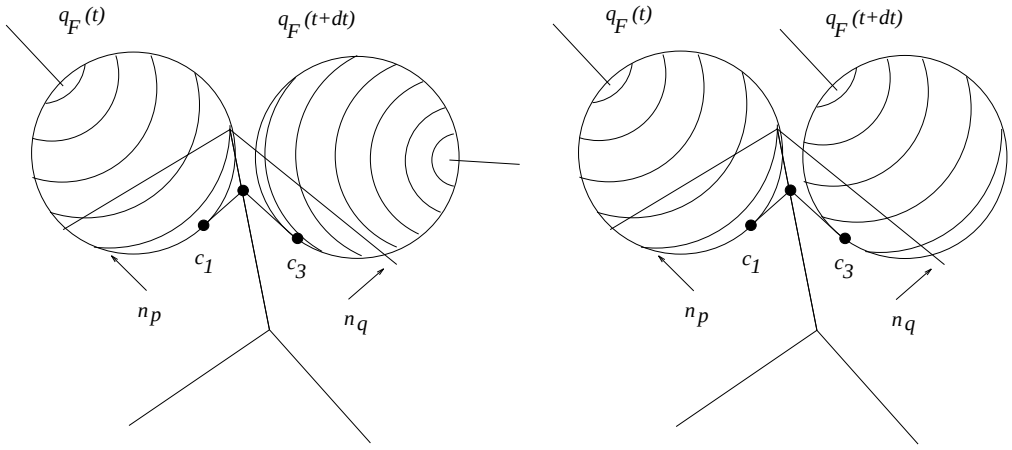

Figure 20: Rolling (top) and sliding (bottom) transition motions between two faces of a polyhedron.

Unit´e de recherche INRIA Lorraine, Technopôle de Nancy-Brabois, Campus scientifique,
615 rue du Jardin Botanique, BP 101, 54600 VILLERS LÈS NANCY
Unit´e de recherche INRIA Rennes, Irisa, Campus universitaire de Beaulieu, 35042 RENNES Cedex
Unit´e de recherche INRIA Rhône-Alpes, 655, avenue de l'Europe, 38330 MONTBONNOT ST MARTIN
Unit´e de recherche INRIA Rocquencourt, Domaine de Voluceau, Rocquencourt, BP 105, 78153 LE CHESNAY Cedex
Unit´e de recherche INRIA Sophia-Antipolis, 2004 route des Lucioles, BP 93, 06902 SOPHIA-ANTIPOLIS Cedex

Éditeur
INRIA, Domaine de Voluceau, Rocquencourt, BP 105, 78153 LE CHESNAY Cedex (France)
http://www.inria.fr
ISSN 0249-6399